Fall 2023

Methylation Patterns Across Tissue Type and Time in Peromyscus leucopus: A Targeted Museum Study

Loryn Smith
Fort Hays State University, lmsmith0998@gmail.com

METHYLATION PATTERNS ACROSS TISSUE TYPE AND TIME IN *PEROMYSCUS LEUCOPUS*: A TARGETED MUSEUM STUDY

A Thesis Presented to the Graduate Faculty

of Fort Hays State University in

Partial Fulfillment of the Requirements for

The Degree of Master of Science

by

Loryn Smith

B.S., Fort Hays State University

Date 11 November, 2023

Approved _____
Major Professor

Approved _____
Dean of the Graduate School

GRADUATE COMMITTEE APPROVAL

The graduate committee of Loryn Smith approves this thesis as meeting partial fulfillment of the requirements for the Degree of Master of Science.

Approved _____
Chair, Graduate Committee

Approved Nicholas Stewart
Committee Member

Approved _____
Committee Member

Approved Tara Phelps-Durr
Committee Member

ABSTRACT

Museum specimens are a vital data source for many types of studies. One relatively new use includes studying methylation patterns. Methylation patterns are a form of epigenetics or how gene expression changes without alteration of the genetic code. These patterns have been examined in many mammals. However, the focus has previously been on overall epigenetic patterns. Few studies have investigated whether methylation patterns differ across tissue types, time, or preservation method. In this study, I compared methylation patterns in muscle, liver, toe pads, and nasal bones from *Peromyscus leucopus* (white-footed mouse) museum specimens collected in 2022, 2018, 2014, and 2008 using reduced-representation bisulfite sequencing. I found methylation patterns were most similar within an individual and there was little to no clustering of methylation patterns based on tissue type or collection year. Additionally, tissue preservation in ethanol had no effect on methylation patterns. This study illuminates the role of tissue type and preservation method in methylation patterns of *P. leucopus* and thereby provides an important resource for researchers seeking to study DNA methylation in museum specimens.

ACKNOWLEDGMENTS

This thesis was made possible through the help and support of many individuals. A very special thanks to Dr. Lorelei Patrick, my advisor, who guided me not only academically, but personally. Thanks to the members of my graduate committee, Dr. Nicholas Stewart, Dr. Alexandra DeCandia, Dr. Tara Phelps-Durr, for reviewing my thesis and making recommendations.

A thanks to the Sternberg Museum of Natural History for providing specimens and tissues. To the Fleharty and Choate Fellowships for supporting me academically and financially, I thank you. The project described was supported by the NIH Grant number P20RR016475 from the INBRE Program of the National Center for Research Resources. Thanks to the Graduate Scholarly Experience for also supporting my thesis through the GSE grants.

TABLE OF CONTENTS

ABSTRACT ii

ACKNOWLEDGMENTS iii

LIST OF TABLES vi

LIST OF FIGURES vii

INTRODUCTION 1

METHODS 7

Selection of Study Organism 7

2022 Field Collection Methods 7

Tissue Sampling and DNA Extraction 8

Amplicon Study 9

RRBS Methods 10

Bioinformatic Analyses 10

Quality Control and Adapter Removal 10

Methylation Calling 11

RRBS Methylation Analysis in R Using methylKit 11

Percent Methylation 12

RESULTS 13

Differential Methylation 14

Percent Methylation 14

What factor influences clustering on a PCA? 15

Does preservation method influence methylation patterns? 17

DISCUSSION 18

TABLES 24

FIGURES 32

REFERENCES 79

LIST OF TABLES

Table Page

Table 1: Specimens 24

Table 2: Primers 25

Table 3: Prefixes 25

Table 4: Identifying Names 25

Table 5: Shapiro-Wilk's Test and Levene's Test 27

Table 6: Kruskal Wallis 29

Table 7: Tukey Test Results 30

Table 8: Two-Way ANOVA 30

LIST OF FIGURES

Figure Page

Figure 1: Predictions 32

Figure 2: Linear Regression Plots 33

Figure 3: Pie Charts 36

Figure 4: Percent Methylation Boxplots 39

Figure 5: PCA All Samples 44

Figure 6: PCA 2022 54

Figure 7: PCA 2018 58

Figure 8: PCA 2014 63

Figure 9: PCA 2008 67

Figure 10: PCA Ethanol vs No Ethanol 71

Figure 11: Bar Plots 76

INTRODUCTION

Museum specimens are an invaluable resource that can be used as a window into the biological past. These collections of specimens can range from skeletons to tissues, and from plants to animals to fungi. Historic specimens can include those collected centuries ago to those collected recently (Burrell et al., 2015). Mammals as a group are a particularly well-preserved taxon that is well-suited for genomic studies (Cook & Light, 2019; Lindblad-Toh, 2020). These specimens provide crucial information – a biological snapshot – of the time and place they were collected which can aid in the conservation and management of species and their environments. Such specimens have been used to examine patterns of evolution, morphology, natural history, phylogenetics, and more recently, epigenetics (Cook & Light, 2019).

Many types of museum specimens can be utilized in the study of genetics and, more specifically, epigenetics. Genetics is the study of heritable changes the DNA sequence (Moore et al., 2013). The genetic sequence refers to the order in which the nucleotide bases adenine, thymine, guanine, and cytosine are found in a strand of DNA. These bases come together to form the double helix seen in DNA. This double helix is wound around proteins called histones and these groups form a nucleosome. A series of condensed nucleosomes that wrap around each other form chromatin. How tightly the nucleosomes or chromatin are wound can affect gene expression (Martin & Zhang, 2007). A genotype codes for the appearance of the phenotype of an individual. The phenotype of an individual is the culmination of all of its expressed characteristics (Nachtomy et al., 2007).

Epigenetics examines heritable changes in gene expression that occur *without* changes to the genetic sequence. One of the epigenetic mechanisms of gene expression is methylation. Methylation of DNA occurs with the addition of a methyl group to the fifth carbon position on

the nucleotide base cytosine, resulting in the formation of 5-methylcytosine. A methyl group is added via a residue of DNA methyltransferases from *S*-adenosyl methionine. The methyltransferases are a series of enzymes that transfer a methyl group via catalytic nucleophilic attack (Lennard, 2010).

Epigenetic methylation is one of the underlying causes of phenotypic plasticity. Phenotypic plasticity is when an individual's developmental or environmental conditions can cause the same genotype to produce different phenotypes. Phenotypes include measurable traits including hair color, eye color, and susceptibility to diseases (Nachtomy et al., 2007). When DNA becomes wound so tightly that there is a loss of gene expression, it is referred to as heterochromatin, which can lead to suppression or expression of different genes and therefore different phenotypes in the individual. When DNA is wound more loosely, called euchromatin, the transcription of the genes in that nucleosome increases, increasing gene expression, resulting in phenotypic differences (Tamaru, 2010). In addition to its role in phenotypic plasticity, changes in methylation patterns have been linked to cancer and other health problems. DNA methylation can lead to the silencing of tumor suppressor genes (Lakshminarasimhan & Liang, 2016) and has also been linked to cardiovascular diseases and nervous disorders (Kandi & Vadakedath, 2015).

Methylation typically occurs on cytosine bases situated next to guanine bases; these are known as CpG sites. CpG islands – long stretches of DNA that contain a higher-than-average number of CpG sites – often contain promoter regions (Blackledge & Klose, 2011). Before DNA can be transcribed to RNA, transcription binding factors must attach to these promoter regions. DNA that is methylated winds more tightly around the histones and nucleosomes, decreasing gene expression because transcription binding factors are not able to reach the promotor regions,

so the DNA is transcribed at lower rates compared to non-methylated regions (Moore et al., 2013).

A variety of methods have been used to quantify epigenetic methylation patterns to better understand their influence on morphology, physiology, ecology, and evolution. One technique gaining popularity in methylation studies is reduced representation bisulfite sequencing (RRBS), which allows for 3-5% of a genome to be examined. RRBS works by using a methylation insensitive restriction enzyme (MspI) to cut the DNA near CpG islands (Gu et al., 2011). Once the DNA has been cut and adapters added, bisulfite conversion takes place. Bisulfite conversion works by converting unmethylated cytosines into uracil then to thymine after PCR. Then, the treated DNA is purified and sequenced on an Illumina platform.

Methylation patterns have been studied in a variety of organisms, but most of the focus has been on model organisms. Model organisms are those that live in the laboratory and have been studied extensively. Examples include *Drosophila* (common fruit fly), *C. elegans* (nematodes), *Homo sapiens* (humans), and *Mus musculus* (mouse) (*Model Organisms | NIH Center for Scientific Review*, n.d.). Non-model organisms typically have not been domesticated or used in clinical studies. Several previous epigenetics studies on non-model organisms have focused on a single tissue type (Crossman et al., 2021; Rubi et al., 2020; Weyrich et al., 2016). One such study used nasal bones of deer mice in the genus *Peromyscus* from museum collections to examine methylation patterns across time (Rubi et al., 2020). They compared changes in methylation between historic and recent populations during an ongoing range expansion. The study was successful in using 76-year-old specimens to extract DNA from bones and perform bisulfite conversion to quantify methylation (Rubi et al., 2020). They were able to investigate

global methylation in specimens of different ages and that the global methylation did not vary among different ages of the specimens.

An increasing number of studies have used methylation patterns of CpG islands to answer a variety of ecological questions in wildlife. For example, stress is hypothesized to affect methylation patterns in mammals (Murgatroyd et al., 2009). A study comparing two killer whale populations examined 25 CpG sites found in three previously studied stress response genes to investigate epigenetic manifestations of stress using skin biopsies collected from free swimming animals (Crossman et al., 2021). The study used two distinct whale populations, the Northern Resident killer whale population and Southern Resident killer whale population in the Pacific Northwest. The researchers found that neither age nor sex affected methylation patterns. Even though the two populations were genetically distinct, they had similar levels of stress based on the methylation patterns of the three genes of interest (Crossman et al., 2021). However, at two of the CpG sites they found different methylation levels consistent with stress exposure in the killer whale populations.

Despite the increasing number of epigenetics studies, many methodological questions remain, including the extent to which methylation patterns differ between tissues within the same individual. A study in humans investigated how tissue types correlated with methylation patterns and gene expression. This study used 12 tissues including sperm, fetal liver, CD4+ lymphocytes, CD8+ lymphocytes, fibroblasts, fetal skeletal muscle, placenta, keratinocytes, melanocytes, skeletal muscle, heart muscle, and liver (Fan & Zhang, 2009); of the 12 tissues used, 11 were somatic. The researchers found that the CpG island methylation patterns in various somatic tissues were extremely similar to each other. They also found the CpG island methylation profiles in germ cells were distinct from somatic cells. This suggests that different tissues share

similar methylation profiles depending on their origin (i.e., somatic or germ cells). In addition, they did not find an obvious relationship between CpG island methylation and gene expression across these tissue types (Fan & Zhang, 2009).

One of the few studies comparing methylation across tissue types in a non-model organism focused on differences in blood, brain, liver, and gonad tissues in the house sparrow (*Passer domesticus*; (Shi, 2021)). The goal of the study was to examine the amount of methylation present in different tissue types between the sexes. The researcher used RRBS to quantify methylation patterns of the different tissues (brain, liver, blood, and gonads) to compare the amounts of methylation between the tissues and blood. Blood is often used to quantify methylation in animals (Macartney-Coxson et al., 2020); however, no one had quantified differences in methylation between blood and tissues. The researcher found that blood had the lowest number of methylated sites compared to the other tissues (Shi, 2021). This suggests that blood may not provide a full picture of the methylation patterns in an individual, so should be used with caution for methylation studies. It also highlights the lack of studies examining differences in methylation patterns across tissues and time for non-model organisms.

Previous studies of non-model organisms typically focus on differences in methylation patterns between different tissues or over differing temporal and spatial gradients (Blake et al., 2020; B. Zhang et al., 2013). Aside from the house sparrow study cited above (Shi, 2021), little research has considered the role of tissue type and time in methylation patterns for any non-model species, thus it is unknown how these factors influence epigenetic studies (Husby, 2022). In addition, little is known about how methylation patterns differ across time or with preservation method, although some researchers have suggested investigating this question should be a priority (Hahn et al., 2020). At the time of writing, there were currently no studies

published that study how ethanol preservation affects methylation patterns. Despite the growing prevalence of methylation studies in model and non-model organisms, including wildlife, there remains open questions and lack of data on best practices. If there are differences in methylation between tissue types, then this should be considered when designing studies. Additionally, if there are differences in methylation patterns between ethanol preserved and fresh specimens, then this should also be considered when designing studies.

This study will bridge these knowledge gaps by examining epigenetic differences in the white-footed mouse, *Peromyscus leucopus*. The main goals were to investigate overall methylation patterns to see if there is a difference across different tissue types, time, and preservation method in museum specimens. If methylation patterns are more similar between tissue types than between individuals, I will observe samples clustering by tissue (Figure 1, upper left); this was the pattern I expected to observe. It would also be plausible for tissues to cluster by similar tissue type, in which case liver and muscle might cluster together but separately from skin and bone (Figure 1, lower left corner). If methylation patterns differ dramatically by year, I would expect four distinct clusters containing all individuals and tissues from a given year (Figure 1, upper right corner). If methylation patterns are similar within an individual but differ between individuals, I would expect to see clustering of tissue samples for each individual specimen (Figure 1, upper right corner). Finally, if ethanol preservation affects methylation patterns, I would expect samples to cluster based on preservation method (Figure 1, lower right corner); this is the pattern I expected to observe.

Another goal of this study was to look at percent methylation for CpG sites and overall total percent methylation. This will give a picture of how well the sequencing worked, regions of the genome that are methylated, if there are differences in the amount of methylation between

tissue types, and an overall view of the amount of methylation present in the samples. None of these have been quantified for the species used in this study.

METHODS

Selection of Study Organism

The white footed mouse, *Peromyscus leucopus,* is a non-model organism because it is found in the wild and has not been domesticated for laboratory studies. This species was chosen because numerous specimens and tissues were available at the Sternberg Museum of Natural History in Hays, Kansas which allowed for sufficient sample sizes for this study. It is an abundant mammal found in the Midwest and throughout Kansas. It can be identified and distinguished from other members of the genus *Peromyscus* by its lack of a bicolored tail, brown body with a white underbelly, long hind foot, lack of grooved incisors, and large ears covered with thin hair. Their habitat preference is woodlands or warm, dry forests. The white-footed mouse can mate throughout the year, but typically does so in the fall and spring (Lackey et al., 1985). The gestation period for offspring is typically 24 to 28 days and number of offspring can range from one to nine with the average number of offspring being four (*Kansas Mammal Atlas*, 2017). Due to the relative quickness of its reproductive state, the white-footed mouse is found in abundance in the Midwest and Kansas which makes it an ideal candidate for this type of study.

2022 Field Collection Methods

Six *Peromyscus leucopus* specimens were collected in October 2022 at a field site at the nature trails near the Sternberg Museum of Natural History (38.89004 N, -99.30061 W). Approximately 100 Sherman traps were set up along 1-4 100 meter transects that followed tree lines. The traps were baited with peanut butter and oatmeal balls; cotton balls were also added to the traps when nightly temperatures were below 50° F. Traps were checked every morning and

reset until six adult *P. leucopus* were captured. These mice were euthanized with chloroform. All trapping and euthanasia were performed with Kansas permit #SC-091-2022 and with FHSU IACUC approval.

Tissue Sampling and DNA Extraction

Bones, muscle, skin, and liver tissue samples preserved at the Sternberg Museum of Natural History were used in this study. The tissues included those from 2022, 2018, 2014, and 2008 collected from around Hays, Kansas, specifically Barton, Ellis, and Russell counties. These tissues and time points were chosen based on their availability and their use as DNA sources in previous studies. The specimens, years, county, sex, and tissue types for this study are summarized in Table 1.

The skin-derived samples came from toe pads, which were still fleshy and have been used for DNA extraction previously on birds (Lutgen & Burri, 2022). Two to three milligrams of tissue from the toe pads were scraped off using a sterilized scalpel blade. A new scalpel blade was used for each sample. The bone-derived samples were from nasal turbinates to minimize damage to the specimen. A pair of tweezers were inserted into the nasal passages and 1.5-4 milligrams of bone was scraped into a tube. The bone samples were put into a -80℃ freezer before being crushed using biomasher tubes before proceeding with DNA extraction. The muscle and liver were preserved in ethanol (the standard tissue preservation method at the Sternberg Museum of Natural History); a 2-5 milligram subsample were taken for each tissue from each specimen. DNA was extracted from all tissue samples following the manufacturer's instructions for the Qiagen DNeasy Blood and Tissue Kit (Qiagen, USA).

The ethanol versus no ethanol study required liver and muscle samples to be immediately DNA extracted following specimen preparation (no ethanol). Then the muscle and liver from the

same individuals were placed in ethanol from November 2022 to May 2023. These samples were extracted using the Qiagen DNeasy Blood and Tissue Kit (Qiagen, USA) following the manufacturer's instructions.

Amplicon Study

The original strategy for this study was to perform amplicon sequencing of one or more CpG island sites. A total of six genes were picked at random from a previously published list (Horvath et al., 2021). Then Kcnn2, Mafb, Nav1, Pax6, Pura, and Taok3 were chosen because they were protein coding, and the area was an exon. The number of CpG sites in each gene varied from 6 – 14. Several of the genes were in fragments and those were assembled to create an approximately 300-base pair (bp) fragment. These fragments were then put into a primer predicting software called Primer3 (*Primer3*, n.d.). The resulting primers were tested using the procedure below.

The six primer sets (Table 2) were tested using Cytiva PurReTaq Ready-To-Go PCR beads under a variety of thermocycler conditions. However, only Mafb was successfully amplified under the following thermocycler conditions: initial denaturation 95℃ for 5 minutes, 35 cycles of denaturation at 94℃ for 30 seconds, annealing at 60℃ for 45 seconds, extension at 72℃ for 1 minute and final extension at 72℃ for 3 minutes with an infinite hold at 4℃.

A bisulfite conversion was done on the DNA using Qiagen's EpiTect Bisulfite Kit to determine if amplification was more successful before or after conversion. DNA from the same samples were used for both treatments. Manufacturer's instructions were followed for the bisulfite conversion process. I found that the concentrations of DNA were higher in the samples that were PCR'd after bisulfite conversion.

This strategy was abandoned after it was realized that RRBS would be the better option. Though, not the cheaper option, RRBS provides more information about methylation patterns compared to individual amplicons.

RRBS Methods

The typical genome size in *Peromyscus leucopus* is approximately 2.5 billion base pairs (*Peromyscus leucopus Genome Assembly*, 2020). RRBS sequences approximately 3-5% of the genome. This equates to approximately 75 million to 125 million base pairs of the genome. The Zymo-Seq RRBS Library Kit (Zymo Research, USA) was used to add indices, perform bisulfite reactions, and prepare the DNA for sequencing, following the manufacturer's instructions. The indices added during library preparation allowed for sample identification in downstream analyses. Samples were sent to Kansas University Genome Core where Illumina sequencing was performed on the NovaSeq 6000 with a read length of 100 bp and paired-end reads.

Bioinformatic Analyses

Quality Control and Adapter Removal – Four FastQ files per sample were received from KU Genomics Core. The samples were demultiplexed prior to making them available for download. The four files consisted of two lanes with reads one and two each, meaning there were forward and reverse reads per lane. These FastQ files were downloaded locally then placed onto Beocat (*Beocat*, 2021), a high-performance computing cluster at Kansas State University. An initial quality control check was performed on the FastQ files using FastQC prior to concatenating the lanes (*FastQC*, n.d.). Reads for each sample that passed the quality control check were concatenated (combined).

Trimmomatic (Bolger et al., 2014) was then used to trim adaptors from the sequences; these adaptor prefixes were taken from the Zymo-Seq RRBS Library Kit and can be found in

Table 3. In addition to trimming, leading and trailing bases were removed as were reads below 50 bp. The sliding window was 4 bases and cutting occurred when the average quality per base dropped below 15. Another FastQC check was performed on the sequences after trimming to ensure that all adapters had been removed.

Methylation Calling – Bismark (Krueger & Andrews, 2011) was then used to assemble the bisulfite converted genome and extract cytosine coverage. The genome preparation took place first using the *Peromyscus leucopus* (UCI_PerLeu_2.1, Oct. 2020) reference genome (*Peromyscus leucopus Genome Assembly*, 2020). Bismark created folders containing the converted genomes (C to T and G to A) that were then indexed using Bowtie2 (Langmead & Salzberg, 2012). After the Bismark alignment took place, the methylation extractor was used. This extracted the methylation from the files. A bedGraph report was then made in preparation for the final step. The final step was using coverage2cytosine to create CpG files that were compatible with R. All the CpG report files were zipped and then downloaded locally.

RRBS Methylation Analysis in R Using methylKit – The methylKit package (Akalin et al., 2012) allows for downstream methylation analysis in R (R Core Team, 2023). The CpG report files from Bismark were converted to methylKit objects with the minimum coverage set to 100 due to the coverage ranging from 1-~1700.

All the samples were merged using the unite function. To ensure all the files had loaded properly, sapply with getCoverageStats was used. Files that did not contain enough sequencing information were removed (Table 4).

A principal component analysis (PCA) was performed to reduce the dimensionality of the data and to visualize how the samples grouped together. The input was percent methylation profiles created by Bismark and the data matrix was formed using the samples and all of the

cytosines present in all of the samples. The first two principal components were plotted for each. These PCA plots were color-coded using different parameters from the sample metadata (e.g., tissue type, kk number, year, sex, county, etc.) and a convex was added to help visualize if and how samples were clustering, by connecting the plotted points for the different parameters.

Differential methylation was initially calculated using the function calculateDiffMeth. Then, to get all differential methylation the function getMethylDiff was used. In order to view differentially methylated regions associated with genes and CpG islands, annotation files in BED format were downloaded from the UCSC genome browser (*UCSC Genome Browser*, n.d.). The following settings were used for gene annotation: selection from group was "Genes and Gene Predictions" and for CpG island annotation the group was "Expression and Regulation", and the track was "CpG Islands." The function annotateWithGeneParts from the R package genomation (Akalin et al., 2015) was used to show target features that overlap with annotations including promoters, exons, introns, and intergenic regions. To annotate CpG islands, the function readFeatureFlank was used with the flanking regions named "shores" and the CpG islands named "CpGi." The percentage of each annotation type was then plotted using pie graphs.

Percent Methylation – For all the samples, CpG percent methylation was extracted from the Bismark files. In addition to CpG islands, methylation can come from an adenine, thymine, or cytosine, which is denoted by CHG and CHH (Jin et al., 2011). Total percent methylation was calculated by adding the total number of methylated Cs in CpG context, total number of methylated Cs in CHG context, and total number of methylated Cs in CHH context and then dividing that number by the total number of Cs analyzed. All the CpGs, CHGs, and CHHs were provided in the Bismark files. To compare tissue type and percent methylation, boxplots were created for CpG percent methylation and total percent methylation using the ggplot2 package

(Wickham et al., 2023). For all the samples a “treatment” was created. This treatment showed the year and/or tissue being analyzed.

A Kruskal Wallis test was performed on CpG percent methylation and tissue type and total percent methylation and tissue type for all the samples. This was to determine if the percent methylation and tissue type had an interaction. A Kruskal Wallis test was performed because Shapiro-Wilk’s test showed the data was not normally distributed (Table 5A). Following the Kruskal Wallis test, a Tukey’s test was performed for both CpG and total percent methylation against tissue type using the package nparcomp (Konietschke et al., 2019). A Tukey’s test was not reported for CpG and total percent methylation and tissue type with years because there were too many interactions to analyze.

To test whether storage medium influenced methylation patterns, a two-way analysis of variance test (ANOVA) was conducted for samples based on CpG percent methylation and total percent methylation. First, the samples had to be split into four categories. Muscle with ethanol, muscle without ethanol, liver with ethanol, and liver without ethanol. Then, the Shapiro-Wilk’s test was performed on each of the categories to test for normality within the samples. Levene’s test was used to test for equal variances within the samples (Table 5B). They both showed normal distribution and variances. Descriptive statistics were used to create barplots for each group using the barplot function from the package gplots (Warnes et al., 2022). Finally, the two-way ANOVA test was performed to determine if the samples were statistically significant from each other using a 0.05 significance level.

RESULTS

This study examined a total of 88 samples; of these, 81 samples were successfully sequenced and met quality control thresholds. Table 4 summarizes the sequences removed and

retained as well as the number of cytosines (Cs) analyzed. The number of Cs analyzed was only weakly correlated with CpG percent methylation (Figure 2A) and total percent methylation (which included CHH and CHG; Figure 2B), which indicated that sequencing coverage did not bias the results. The samples preserved without ethanol were excluded from analyses where all the samples were examined; they were only analyzed when addressing preservation.

Differential Methylation – Differential methylation was mapped to annotated regions of the genome to determine where in gene regions methylation occurred. CpG percent methylation annotation shows 56% mapping to CpG islands and 44% mapping to other regions (Figure 3A). Differential methylation annotation for different regions of the genome shows 33% mapping to promoters, 44% mapping to intergenic regions, 22% mapping to introns, and 0% mapping to exons (Figure 3B).

Percent Methylation – CpG and total percent methylation were compared to determine if these differed by tissue type and year (Figure 4). There were significant differences between tissue types when tissues from each year were analyzed together for both CpG percent methylation and total percent methylation (Figures 4A and Figure 4B and Table 6A). Liver and muscle had significantly higher CpG percent methylation based on a Tukey test (Table 7). For total percent methylation (Figure 4D), liver was significantly more methylated than the other tissues, but there were no differences in percent methylation among bone, liver, or skin based on a Tukey test (Table 7).

There was more variation for CpG percent methylation than there was for total percent methylation as indicated by the shape and location of the boxes in Figures 4C and Figure 4D, but Kruskal-Wallis tests indicated there were significant differences for both (Table 6B). Liver and muscle tissues collected in 2008 had the highest CpG percent methylation (medians near 40%)

while skin from 2008 specimens had the lowest CpG percent methylation (medians near 20%; Figure 4C). This trend was also observed for total percent methylation, but the medians were lower, near 10% for 2008 liver and muscle and 5% for skin.

What factor influences clustering on a PCA? – The first two components of the PCA for all the samples (except no ethanol) analyzed together accounted for 82.32% of the variation (Figure 5). To visualize if and how samples clustered, points and ellipses were color-coded based on sample characteristics. Points that cluster together are more similar to each other compared to points more distant in principal component space. Clustering was most apparent when samples were color-coded by individual sample (KK number). However, there was much overlap between many of the individuals (Figure 5A).

Clustering was absent or less apparent when other sample characteristics were highlighted. When samples were colored by tissue type, all the ellipses overlapped (Figure 5B). Similarly, complete overlap was also observed when samples were color-coded by sex (Figure 5C). Males have a much larger ellipse than the females as there were more males sampled than females. When points and ellipses were color-coded by year, there was again overlap and no discernable clustering (Figure 5D). Clustering was not observed when color-coded by germ layers (i.e., endoderm, mesoderm, and ectoderm; Figure 5E). There was also no clustering when grouping internal organ sequences separately from bone and skins (Figure 5F). Additionally, when county was color-coded, there was overlap and no clustering (Figure 5G). When individual was color-coded and tissue types were given different symbol shapes, the tissue types were not close to each other in principal component space, nor did individuals have similar relative locations of tissues (Figure 5H), meaning that across individuals, bone for example, did not fall

in the same location of each ellipse. Individuals collected in the same year were found across principal components space, indicating that year did not affect methylation patterns (Figure 5I).

In order to more easily visualize variation in epigenetic methylation within and among individuals, PCAs were run separately for individuals collected from each year sampled. The first two components of the PCAs for the 2022 samples accounted for 69.35% of the variation (Figure 6). Clustering by individual can be seen with some overlap between KK_3734 and KK_3738 and some overlap with KK_3735 and KK_3737 (Figure 6A). There was extensive overlap among samples when tissue type is color-coded (Figure 6B). When sex was examined, the male ellipse completely encompassed the female sample from 2022 (Figure 6C). All the samples from this year were from the same county, thus no PCA graph showing county was created.

The first two components of the PCAs for the 2018 samples accounted for 66.59% of the variation (Figure 7). There was clear clustering by individual with no overlap among individuals (Figure 7A). When tissue type was the focus, there was near complete overlap of tissue types with no clustering between the tissue types (Figure 7B). The sexes overlapped slightly (Figure 7C), and when county is graphed, there was clustering (Figure 7D).

The first two components of the PCAs for the 2014 samples accounted for 56.75% of the variation (Figure 8). Because there was not a full complement of tissues for each individual from this year, it was difficult to assess individual-based clustering and the graphs should be interpreted with caution. It appeared that there was some clustering with little overlap between KK_2927 and KK_2930 (Figure 8A). There were mostly liver tissues for this year which overlapped slightly on the toe pad samples (Figure 8B). The sexes overlapped with each other (Figure 8C). These samples all came from the same county, so no PCA was graphed.

The first two components of the PCAs for the 2008 samples accounted for 78.92% of the variation (Figure 9). There was some clustering by individual but extensive overlap between KK_2034 and KK_2035 and slight overlap with KK_2149, KK_2150, and KK_2034 (Figure 9A). However, much more clustering was observed for individuals compared to tissue type (Figure 9B) and sex (Figure 9C), both of which exhibited extensive overlap. The samples from this year all came from the same county and therefore no PCA was created.

Does preservation method influence methylation patterns? To determine whether preservation method influenced methylation patterns, a PCA for ethanol versus no ethanol can be seen in Figure 10. The first two components of the PCAs accounted for 70.19% of the variation (Figure 10). There was clear clustering happening by individuals, as observed in the other samples (Figure 10A), but not by tissue type (Figure 10B) or sex (Figure 10C). Most importantly, there was extensive overlap between tissues preserved in ethanol versus no ethanol (Figure 10D).

The results of the two-way ANOVAs indicated there were no significant differences in CpG percent methylation and total percent methylation between groups that were individually analyzed (i.e., ethanol and tissue type: Table 8; Figure 11). The two-way ANOVA did show a significant difference in CpG percent methylation when the interaction was tested between ethanol and tissue type (Table 8).

Total percent methylation was also analyzed using the same four categories. The Shapiro-Wilk's and Levene's test showed that all were above the significance level (0.05; Table 5B). This showed normality and variance within the samples. The bar plot for the means and standard deviation shows almost the same percent methylation between the different treatments (Figure

11B). The two-way ANOVA test showed no significant difference in the percent methylation levels between ethanol and no ethanol, tissue type, and their interaction (Table 8).

DISCUSSION

This study is among the first to examine whether time since collection, tissue type, and preservation method influence methylation patterns in a non-model mammal. I found that samples from the same specimen clustered most strongly and did not cluster by tissue type, time since collection, sex, or any other metric for which metadata were available. More evidence of this trend can be seen when percent methylation levels were examined per tissue type in that there was no difference in the percent methylation levels. These findings were different from my initial prediction, based on previous studies, that samples would cluster by tissue. Additionally, preservation method also did not influence methylation patterns. This means ethanol as a preservative has no effect on methylation levels.

There are several possible explanations for why the samples clustered by individual. As mentioned earlier, stress is hypothesized to affect methylation patterns (Murgatroyd et al., 2009). An individual's stress levels could influence how much methylation is present in the tissues. Individuals are exposed to differing stress levels due to many environmental factors beyond the control of researchers using museum specimens. Such environmental stressors could include drought, temperatures, and food/resource availability. Other studies have found that anthropogenic disturbance, resource availability, and early life stress, including level of maternal care and maternal rank, can influence methylation patterns for an individual animal (Francis & Meaney, 1999; Laubach et al., 2019; Murgatroyd et al., 2009), although it is unknown how long these methylation patterns persist within an individual or whether tissues within an individual

become differentially methylated. The present study suggests this must be the case, but more research on controlled populations would be needed to confirm this supposition.

Another explanation for clustering of methylation patterns by individual is that this phenomenon is unique to mammal museum specimens. This might be a possible explanation, but until more studies are done, we cannot know this yet. Previous studies in humans have found differences in methylation patterns between tissues (Fan & Zhang, 2009; Lokk et al., 2014). The Lokk et al. study found a difference in methylation patterns between 17 somatic tissues and the Fan & Zhang study found methylation profiles being similar between 11 somatic tissues. Humans are model organisms; therefore, these studies should be examined with caution when comparing them to a non-model organism because we don't know how methylation patterns for model organisms and non-model organisms compare. This reinforces my assertion that more studies need to be done on other mammalian museum specimens to see how these conflicting studies compare to other species.

CpG islands are typically found in promoter regions but can be found in other regions of the genome as well (Blackledge & Klose, 2011). RRBS sequencing can be biased towards promoters since so many CpG islands are associated with them (Lim et al., 2019). In this study, I found that there was little bias towards promoters, which was unexpected. There was, however, a higher amount of CpG islands found in intergenic regions. Intergenic regions are regions that are distally located to genes, meaning they are between genes (Cain et al., 2022). It is unclear why there is a bias towards intergenic regions when most studies find a higher number of CpG islands in promoter regions (Hughes et al., 2020). A possible explanation for this is that there were not distinct distinguishing features when the genome was previously annotated for promoters and intergenic regions.

In keeping with the other *Peromyscus* study (Rubi et al., 2020), this study found no evidence for consistent changes in methylation patterns based on time since collection. Methylation patterns for this study were consistent and sufficient data was still obtained for the samples from 2008. Methylation patterns did not cluster by year, but by individual. This study, like the previous *Peromyscus* study, was successful in extracting DNA and bisulfite converting the DNA in museum specimens.

It is important that the samples cluster by individual specimens because that means that cytosine methylation studies should not be influenced by which tissue type is chosen. Each tissue type will be representative of the methylation patterns of the individual. Though researchers should attempt to use the same tissue types within an experiment to reduce variability, this study shows that the tissue type chosen matters less than the individual does. During specimen preparation, it is typical to take several organs (e.g., liver, muscle, and heart), dry out the skin, and clean the skull. However, this limits the number of studies that can be done on different tissue types. It is often limited to which tissues the preparator decided to take at the time of preparation. This study demonstrates that high quality DNA can be extracted from all of these tissues. However, some consistency in preserving different tissue types is valuable. Some of my samples did not have tissues available because the preparator did not take them. This limits the number of tissues that can be studied in museum specimens and limited some of the comparisons I was able to make.

There were several limitations of this study. First, RRBS only represents a portion of the genome; it is possible that the methylation patterns differed in parts of the genome that were not represented in the segments that were sequenced. Whole genome bisulfite sequencing could have

alleviated this issue and provided the whole view of genome wide methylation; however, this technique was not used due to budget constraints.

Another limitation was that some samples did not have sufficient sequencing data for analysis. Although I am confident in the results presented, had those samples worked, several of the PCA graphs would have had the full complement of four points per individual.

Additionally, the specimens collected in 2014 and 2018 only had liver tissues collected at the time they were prepared, but not muscle. Ideally all the tissues would have been consistent across all time points. It would have also been ideal that all the specimens came from the same sex and county. These could have influenced the results, although this is doubtful given the extensive overlap among the samples. The exception is the samples from 2018, which clustered by individual and by county. Although it is impossible to know with certainty why this is the case, it is possible that the individuals from the different counties experienced different environmental stress regimes as discussed above.

A future direction of this research could be to create an epigenetic clock. This "clock" can be used to predict the age of an individual, although such clocks can vary between individuals. Aging is a naturally occurring process characterized by the accumulation of cellular damage over time, which can be regulated by chemical changes such as methylation. Thus, an epigenetic clock, using CpG islands as indicators, has been created for humans and other animals that can predict the actual age of an individual (De Paoli-Iseppi et al., 2017; Robeck et al., 2023; Wright et al., 2018; J. Zhang et al., 2021). Different types of tissues can age differently which is why multiple tissues are needed to create the clock. Despite this being a promising future direction of the study, "ground-truthing" is necessary, meaning individuals of known ages are needed. This limits its utility for wild-caught specimens, particularly if no morphological

features, like tooth wear, are available to determine an individual's age; it is currently impossible to age *P. leucopus* using such means.

In the future, I suggest performing whole genome bisulfite sequencing on the samples to see if they still cluster by individual specimens; I hypothesize that they still will. Though RRBS is only a portion of the genome its purpose is to still represent the genome. This is why I hypothesize that in museum specimens clustering by individual will still be seen when whole genome bisulfite sequencing is used.

More research in the future should be done to see if this study holds up in other mammals; particularly those in museum specimens. Since there has been a growing amount of research in museum specimens, it is important to see how this study, finding that there was clustering by individual, holds up in other mammals. This study goes back to 2008 and it is known that in bone methylation patterns hold up for at least 76 years (Rubi et al., 2020). So, it would be interesting to see how much further into the past methylation patterns are maintained in tissues, particularly those preserved in ethanol.

Finally, future studies should examine gene ontology. Gene ontology (GO) is the process of describing gene products and their functions (Ashburner et al., 2000). GO analysis or annotation provides a picture of how methylation patterns can influence gene expression. By using GO analysis for methylation patterns, gene products and their functions associated with CpG islands can be investigated. There are several programs that will take an input of locations and output a list of known gene associations and their functions (Kolberg et al., 2023; Maksimovic et al., 2021). This can tell us the locations of what is being methylated and how it is correlated with functions or phenotypes within an individual.

This study is important because it addresses a knowledge gap in wildlife epigenetics. Since there was no variation in methylation patterns across tissue types, future researchers may choose whatever available tissue type best suits their research question. Additionally, it is very important that no variation in methylation patterns was found between ethanol versus no ethanol samples. This means that methylation holds up (at the very least) since 2008, and I suspect further, in tissues preserved in ethanol. Again, the importance of this is the key to future methylation studies being done on museum specimens. Museums preserve a wealth of biological specimens collected across vast temporal and spatial scales; this study shows that if a researcher should want to use them to examine things like the influence of climate change or range expansion on methylation, they should be able to regardless of the deposition of the specimen.

TABLES

Table 1: Specimens

Tissue (KK) number, Sternberg Natural History Museum (FHSM) specimen accession number, collection year, collection county, and sex for specimens used in this study. The tissue types used from each specimen are indicated by "X" in the corresponding column. Specimens from 2022 will be given an FHSM number when they are cataloged into the collection.

KK	FHSM	Year	County	Sex	Muscle	Liver	Skin	Skull
2032	41623	2008	Russell	M	X	X	X	X
2033	41624	2008	Russell	M	X	X	X	X
2034	41625	2008	Russell	M	X	X	X	X
2035	41626	2008	Russell	F	X	X	X	X
2149	41693	2008	Ellis	F	X	X	X	X
2150	39006	2008	Ellis	F	X	X	X	X
2700	42351	2014	Ellis	F		X	X	X
2886	42753	2014	Ellis	F		X	X	X
2892	42635	2014	Ellis	M		X	X	
2915	42394	2014	Ellis	M		X	X	X
2927	42386	2014	Ellis	F		X	X	
2930	42419	2014	Ellis	M		X	X	X
3572	43350	2018	Barton	M		X		X
3573	43430	2018	Barton	M		X		X
3574	43302	2018	Barton	F		X		X
3602	43293	2018	Russell	M		X	X	X
3619	43317	2018	Ellis	F		X	X	X
3669	43309	2018	Russell	F		X	X	X
3734		2022	Ellis	M	X	X	X	X
3737		2022	Ellis	F	X	X	X	X
3735		2022	Ellis	M	X	X	X	X
3738		2022	Ellis	M	X	X	X	X
3740		2022	Ellis	M	X	X	X	X
3744		2022	Ellis	M	X	X	X	X

Table 2: Primers

Primer sets with their respective primer sequences, locations, and number of CpG sites.

Gene/Primer Name	Location from NCBI	# CpG Sites	LEFT Sequence	RIGHT Sequence
Kcnn2	Chr19	11	CATGCCCATTGTTTTGGTG	GCAATGCAGGTGTGAGGAG
Mafb	Chr4	12	CAGCAGAAACATCACCTGGA	ACACAGGACAGGGAGTCTGG
Nav1	Chr15	9	GGGCCAGCTTACCAACATAG	GTAGGTGGAAGAGGCACTGG
Pax6	Chr4	6	GTCCATCTTTGCTTGGGAAA	CTTGTGTAGGTTGCCCTGGT
Pura	Chr19	13	CGACTTCATCGAGCACTACG	GAACTCGATGAGCCCCTGT
Taok3	Chr23	14	TGTCAGGTTACAAGCGGATG	GCTACCTTCGCCTCCTTTTC

Table 3: Prefixes

Prefixes and their reverse compliments use in the TrueSeq3-PE file for Trimmomatic.

	prefix	prefix rc
1	AGATCGGAAGAGCACACGTCTGAACTCCAGTCA	TGACTGGAGTTCAGACGTGTGCTCTTCCGATCT
2	AGATCGGAAGAGCGTCGTGTAGGGAAAGAGTGT	ACACTCTTTCCCTACACGACGCTCTTCCGATCT

Table 4: Identifying Names

The identifying name used for analysis along with the total number of samples that were analyzed and the total number of samples that were not analyzed. The Table also shows the number of cytosines (Cs) analyzed.

Identifying Name	Removed	Number of Cs Analyzed
2008_M_2032		13306924
2008_M_2033		21290700
2008_M_2034		20599086
2008_M_2035		16496326
2008_M_2149		17555093
2008_M_2150		24649693
2008_L_2032		37067783
2008_L_2033		16593482
2008_L_2034		9400509
2008_L_2035		16185477
2008_L_2149		16525249
2008_L_2150		27418384

2008_T_2032		17762051
2008_T_2033		20120488
2008_T_2034		20474504
2008_T_2035		16405168
2008_T_2149		17031508
2008_T_2150		26075619
2014_T_2915		37437061
2014_T_2927		14690353
2014_T_2930		33603368
2018_T_3602		27733966
2018_T_3619		25287257
2018_T_3669		12043702
2014_L_2700		8916039
2014_L_2886		26705698
2014_L_2892		29408135
2014_L_2915		10246228
2014_L_2927		22529771
2014_L_2930		27020889
2018_L_3572		24567425
2018_L_3573		38028984
2018_L_3574		27074670
2018_L_3602		27638531
2018_L_3619		33128556
2018_L_3669		28101791
2008_B_2032		26819697
2008_B_2033		32361339
2008_B_2034		19394991
2008_B_2035		13361178
2008_B_2149		34775201
2008_B_2150		27900244
2018_B_3572		19463704
2018_B_3573		12266448
2018_B_3574		21603987
2018_B_3602		12295243
2018_B_3619		25625051
2018_B_3669		11186709
2014_B_2700	x	390766
2014_B_2886		30304916
2014_B_2915	x	18700
2014_B_2930	x	48731
2022_T_3744		36552432
2022_T_3738		41993431
2022_T_3740	x	77

2022_T_3734		25986146
2022_T_3735		25873740
2022_T_3737	x	1048998
2022_M_3744_NE		33150014
2022_M_3738_NE		24957785
2022_M_3740_NE		32975115
2022_M_3734_NE		22630623
2022_M_3735_NE		10250926
2022_M_3737_NE		20822887
2022_L_3744_NE		33268011
2022_L_3738_NE		19015113
2022_L_3740_NE		28510003
2022_L_3734_NE		23820629
2022_L_3735_NE		31945302
2022_L_3737_NE	x	42688087
2022_M_3744		10305850
2022_M_3738		24424716
2022_M_3740		35809005
2022_M_3734		35651758
2022_M_3735		12914937
2022_M_3737		39319528
2022_L_3744		33211339
2022_L_3738		25726140
2022_L_3740		25143822
2022_L_3734		40290828
2022_L_3735		23910502
2022_L_3737	x	815848
2022_B_3744		32811991
2022_B_3738		23500078
2022_B_3740		40078459
2022_B_3734		22127574
2022_B_3735		22296322
2022_B_3737		22353204
total number of samples analyzed	81	
total number of samples not analyzed	7	

Table 5: Shapiro-Wilk's Test and Levene's Test

A) CpG percent methylation and total percent methylation with p-values for Shapiro-Wilk's test for all the samples. B) CpG percent methylation and total percent methylation with p-values and descriptive statistics for ethanol vs no ethanol.

A)

CpG Percent Methylation		
Shapiro-Wilk's Test		
	W	p-value
muscle	0.86495	0.0147
liver	0.93676	0.0825
bone	0.78174	0.000628
toe pads	0.96043	0.6697
Total Percent Methylation		
Shapiro-Wilk's Test		
	W	p-value
muscle	0.70456	9.03E-05
liver	0.88703	0.004859
bone	0.84304	0.005179
toe pads	0.9865	0.995

B)

CpG Percent Methylation			
Shapiro-Wilk's Test			
	W	p-value	
muscle ethanol	0.93195	0.5953	
muscle no ethanol	0.96355	0.8467	
liver ethanol	0.85257	0.2028	
liver no ethanol	0.83932	0.1631	
Levene's Test			
	F value	pr(>F)	
all	1.5633	0.2329	
Descriptive Statistics			
	N	Means	SD
muscle ethanol	6	33.68333	3.611879
muscle no ethanol	6	30.86667	0.553775
liver ethanol	5	29.42	2.901207
liver no ethanol	5	37.08	4.543347
Total Percent Methylation			

Shapiro-Wilk's Test			
	W	p-value	
muscle ethanol	0.84863	0.1534	
muscle no ethanol	0.81857	0.08577	
liver ethanol	0.85378	0.2068	
liver no ethanol	0.83325	0.1471	
Levene's Test			
	F value	pr(>F)	
all	2.3471	0.1069	
Descriptive Statistics			
	N	Means	SD
muscle ethanol	6	11.10683	4.049555
muscle no ethanol	6	9.519835	1.430796
liver ethanol	5	8.215543	0.546005
liver no ethanol	5	9.082652	0.919285

Table 6: Kruskal Wallis

A) Test for CpG and total percent methylation against tissue type. The significance level was 0.05. Both CpG and total percent methylation have a p-value below the significance level. B) Test for CpG and total percent methylation against tissue types/years. The significance level was 0.05. Both CpG and total percent methylation have a p-value below the significance level.

A)

CpG Percent Methylation and Tissue Type		
Kruskal Wallis		
chi-squared	df	p-value
20.92	3	0.0001094
Total Percent Methylation and Tissue Type		
Kruskal Wallis		
chi-squared	df	p-value
20.226	3	0.0001524

B)

CpG Percent Methylation and Tissues/Years		
Kruskal Wallis		
chi-squared	df	p-value
53.698	13	6.83E-07
Total Percent Methylation and Tissues/Years		
Kruskal Wallis		
chi-squared	df	p-value
42.244	13	5.97E-05

Table 7: Tukey Test Results

Tukey results for CpG and total percent methylation against tissue type. The significance level was 0.05. CpG Percent Methylation and Tissue Type) B-M and M-T showed a significant difference. Total Percent Methylation and Tissue Type) B-M, L-M, M-T showed a significant difference.

CpG Percent Methylation and Tissue Type		
Tukey		
comparison	statistic	p-value
B-L	2.4236517	0.0752894
B-M	3.2676512	0.005859554
B-T	-0.5664705	0.972214131
L-M	1.6613754	0.365515258
L-T	-2.5488375	0.053580971
M-T	-3.4059656	0.003681426
Total Percent Methylation and Tissue Type		
Tukey		
comparison	statistic	p-value
B-L	0.3686877	0.994613545
B-M	3.0929932	0.009084398
B-T	-1.6602611	0.36428277
L-M	2.7631676	0.029814172
L-T	-2.2447917	0.116737965
M-T	-3.9990185	0.000247006

Table 8: Two-Way ANOVA

Two-way ANOVA results for both CpG percent methylation and total percent methylation.

CpG Percent Methylation					
ANOVA					
	Df	Sum Sq	Mean Sq	F value	Pr(>F)
Ethanol$Ethanol	1	20.82	20.82	2048	0.16959
Ethanol$Tissue_Type	1	5.19	5.19	0.51	0.48429
Ethanol$Ethanol: Ethanol$Tissue_Type	1	149.67	149.67	14.722	0.00121
Residuals	18	183	10.17		
Total Percent Methylation					
ANOVA					
	Df	Sum Sq	Mean Sq	F value	Pr(>F)
Ethanol$Ethanol	1	1.22	1.223	0.227	0.639
Ethanol$Tissue_Type	1	15.11	15.107	2.809	0.111
Ethanol$Ethanol: Ethanol$Tissue_Type	1	8.21	8.213	1.527	0.232
Residuals	18	96.8	5.378		

FIGURES

Figure 1: Predictions

Predictions of outcomes for this study for a PCA. Each dot represents an individual and a tissue type. Upper Left) Clustering by tissue type. Lower Left) Internal organs are similar i.e., muscle and liver cluster together separately from bone and skull. Upper Right) Two outcomes for the study being by year or individuals. Clustering by year would be four separate groups and for a given year individual clustering would have six groups. Lower Right) Ethanol versus no ethanol study. Ethanol clusters independently of no ethanol.

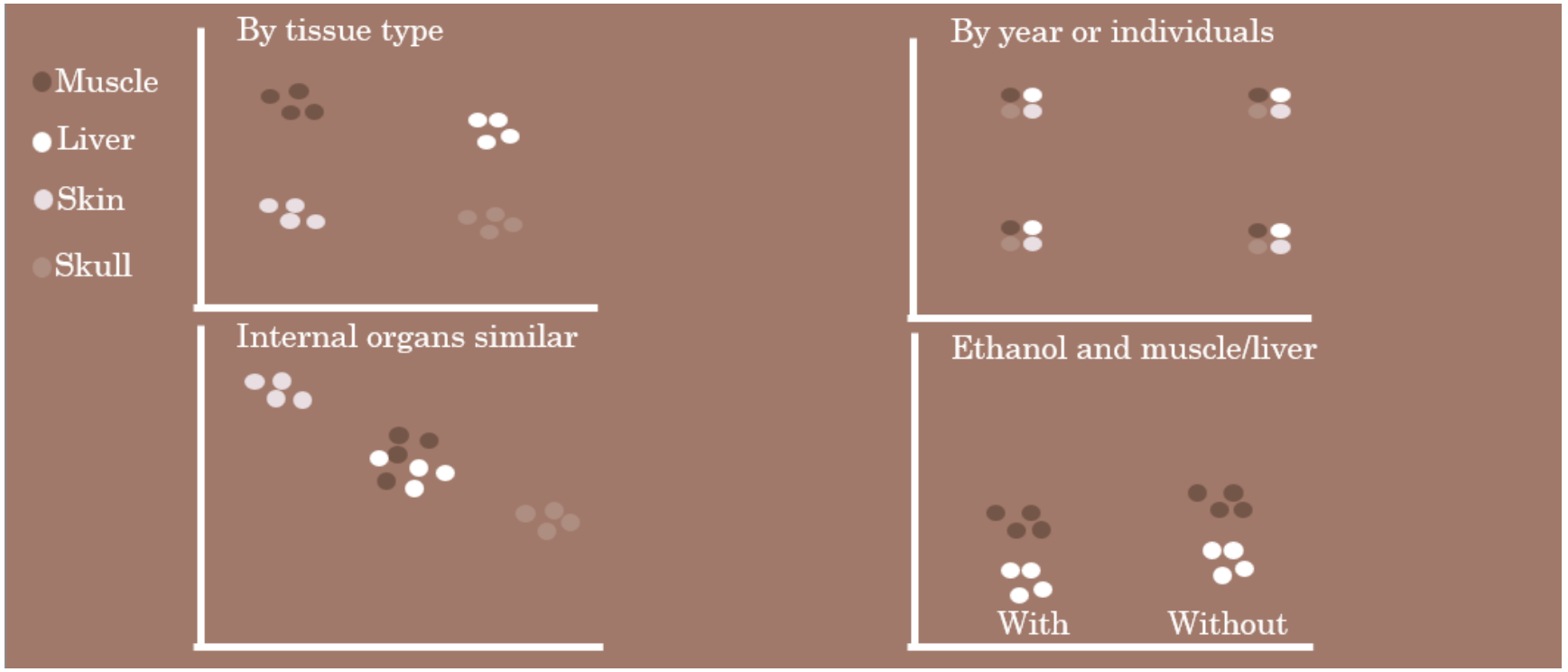

Figure 2: Linear Regression Plots

A) CpG percent methylation graphed against total number of Cs analyzed. B) Total percent methylation graphed against total number of Cs analyzed.

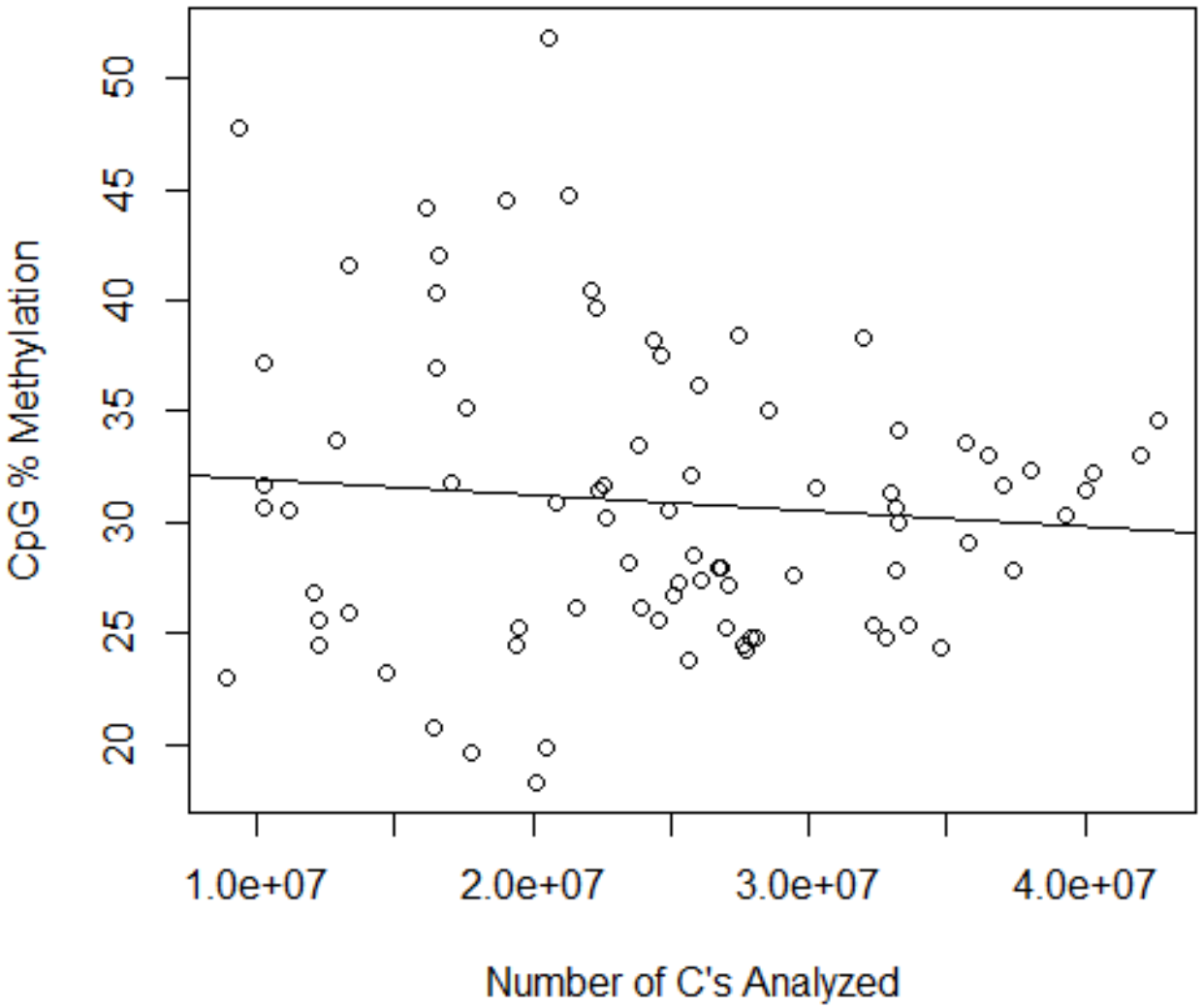
CpG % Methylation
20
25
30
35
40
45
50
1.0e+07
2.0e+07
3.0e+07
4.0e+07
Number of C's Analyzed

A)

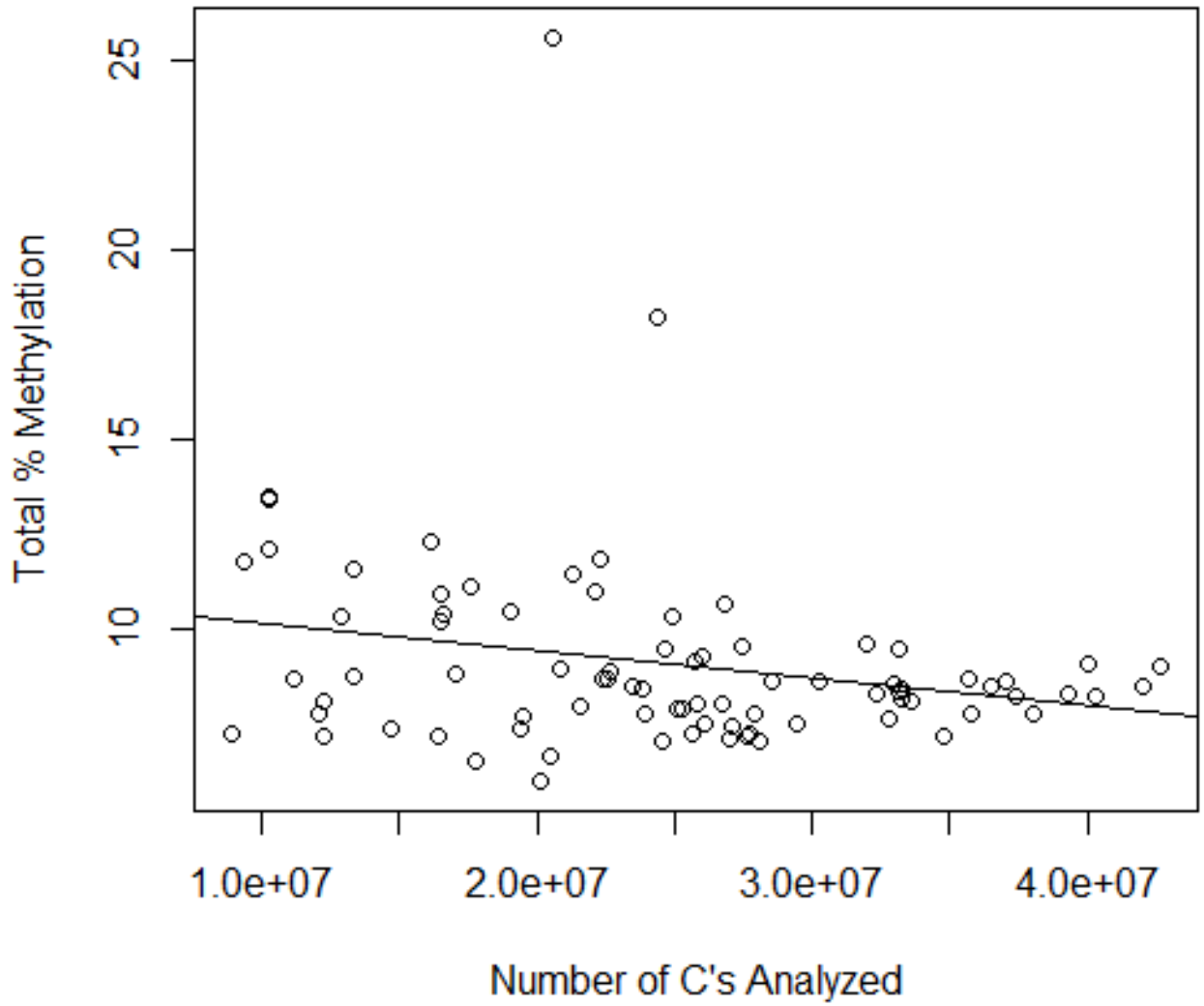
Total % Methylation
25
20
15
10
1.0e+07
2.0e+07
3.0e+07
4.0e+07
Number of C's Analyzed

B)

Figure 3: Pie Charts

Differential methylation annotation. A) Differential CpG methylation annotation B) Differential methylation annotation for different regions in the genome

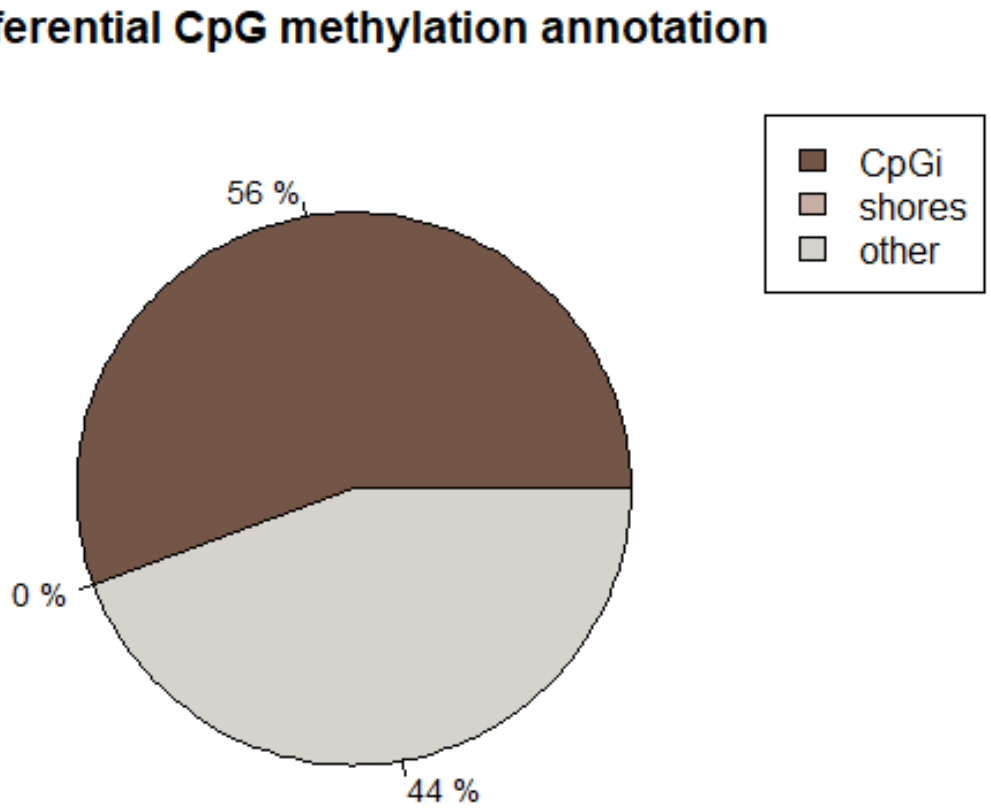
differential CpG methylation annotation
CpGi
shores
other
56 %
0 %
44 %

A)

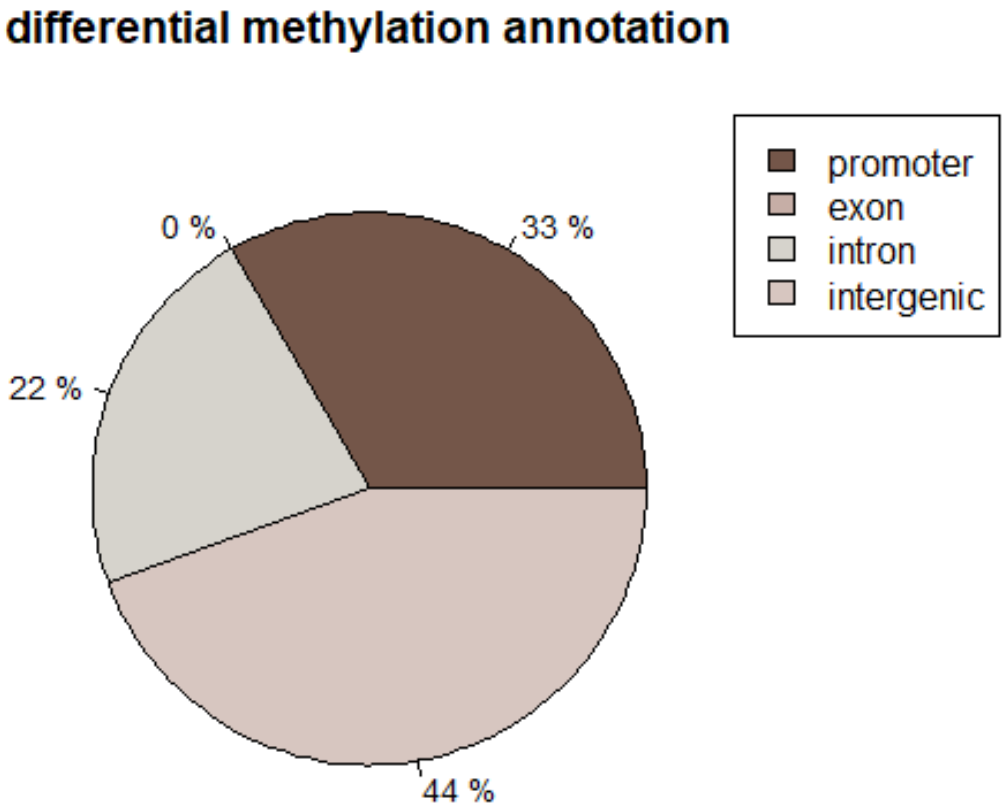
differential methylation annotation
promoter
exon
intron
intergenic
0 %
33 %
22 %
44 %

B)

Figure 4: Percent Methylation Boxplots

A) CpG Percent Methylation according to tissue type and year B) Total Percent Methylation according to tissue type and year C) CpG percent methylation according to tissue type. D) Total percent methylation according to tissue type

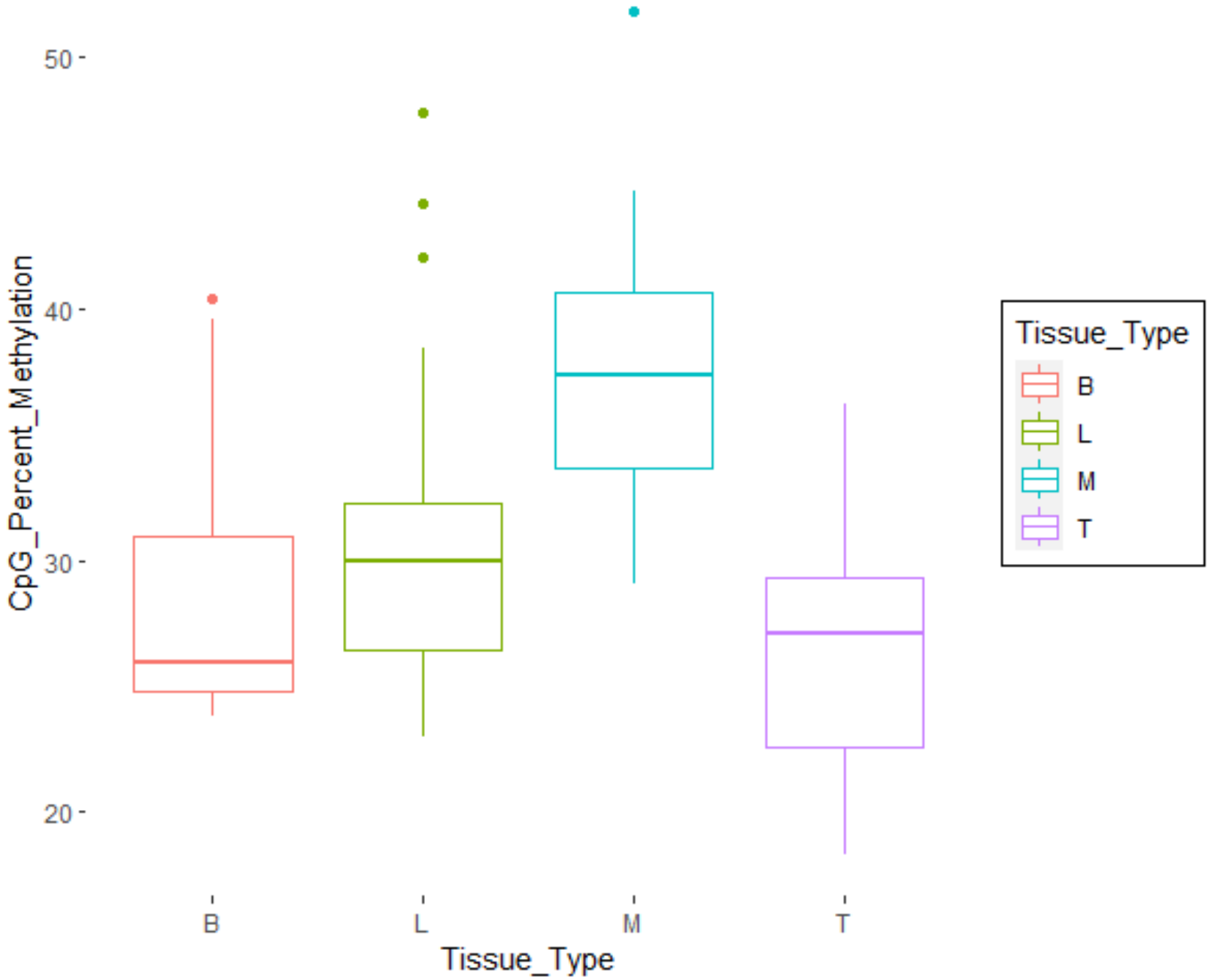
50
40
30
20
CpG_Percent_Methylation
B
L
M
T
Tissue_Type
Tissue_Type
B
L
M
T

A)

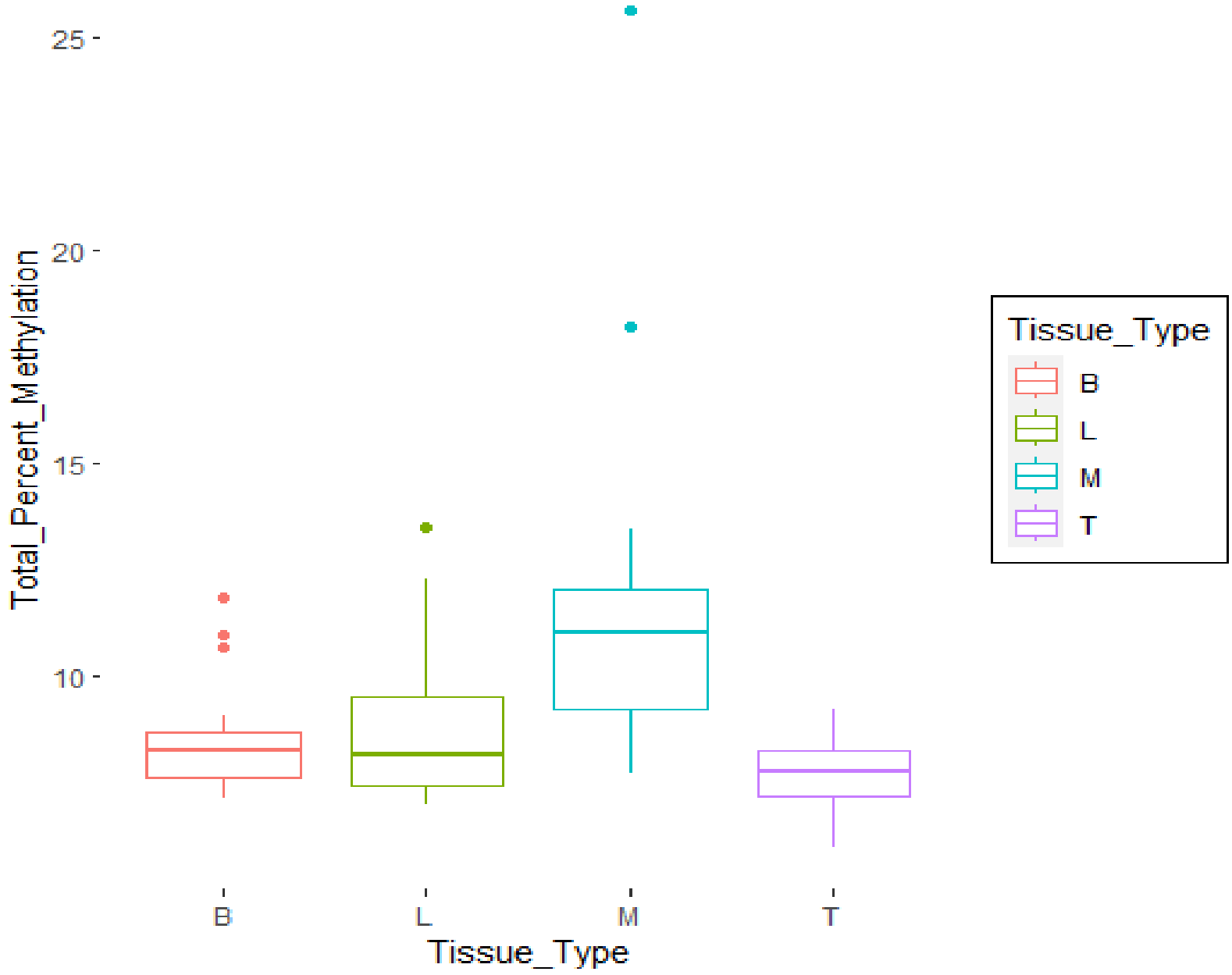
Total_Percent_Methylation
25
20
15
10
B
L
M
T
Tissue_Type
Tissue_Type
B
L
M
T

B)

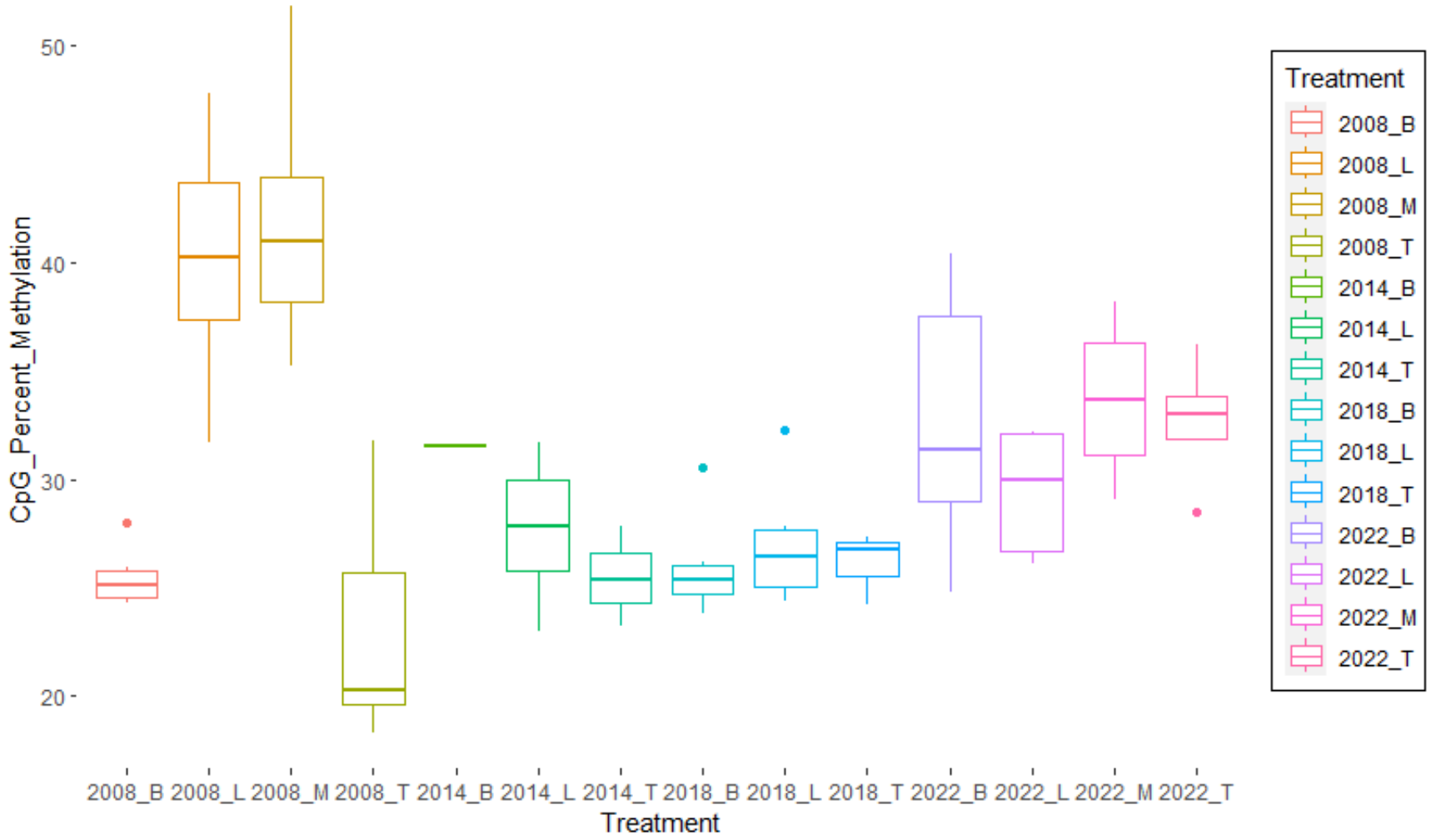
CpG_Percent_Methylation
50
40
30
20
2008_B
2008_L
2008_M
2008_T
2014_B
2014_L
2014_T
2018_B
2018_L
2018_T
2022_B
2022_L
2022_M
2022_T
Treatment
Treatment
2008_B
2008_L
2008_M
2008_T
2014_B
2014_L
2014_T
2018_B
2018_L
2018_T
2022_B
2022_L
2022_M
2022_T

C)

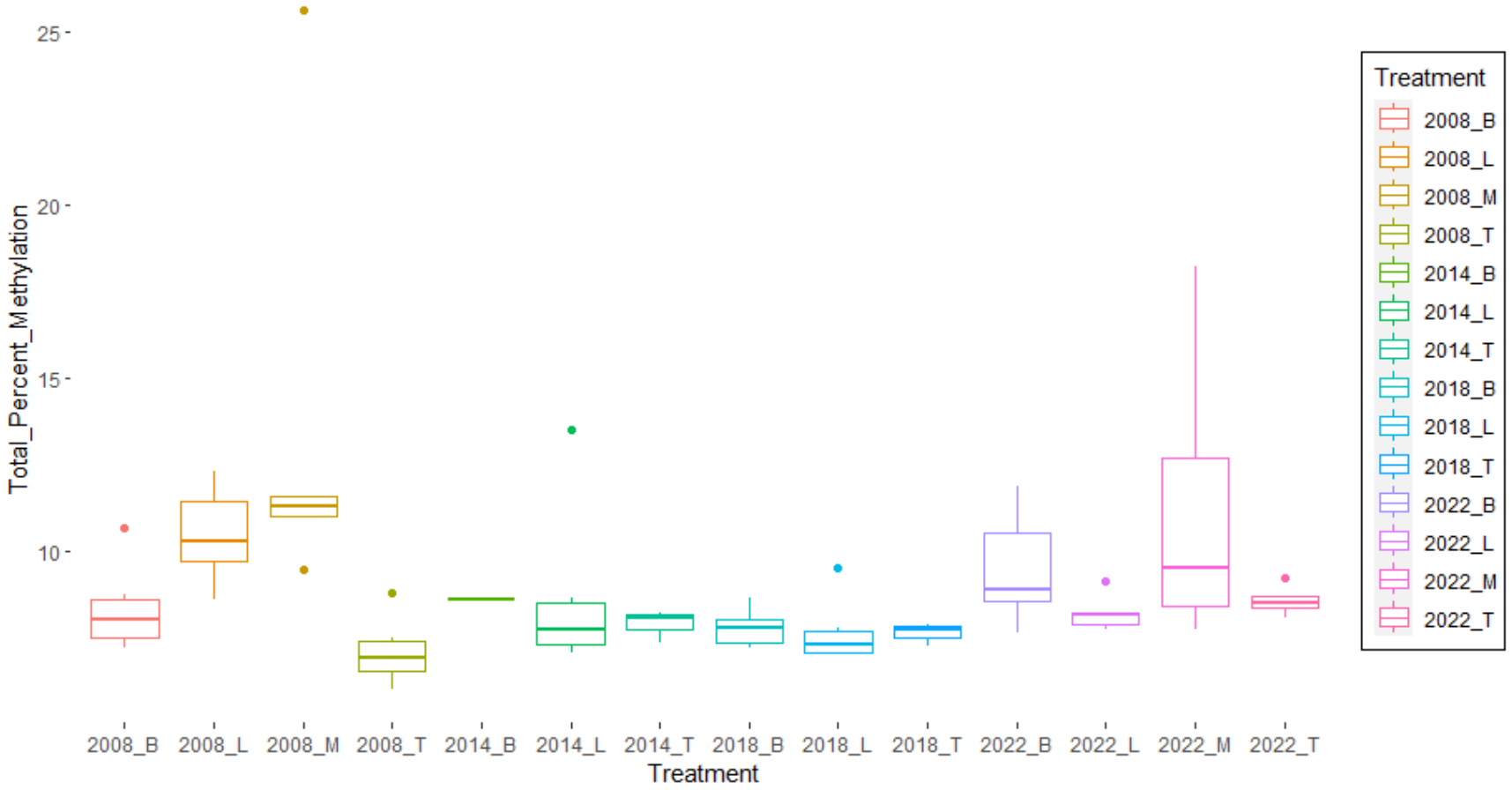
Total_Percent_Methylation
25
20
15
10
2008_B
2008_L
2008_M
2008_T
2014_B
2014_L
2014_T
2018_B
2018_L
2018_T
2022_B
2022_L
2022_M
2022_T
Treatment
Treatment
2008_B
2008_L
2008_M
2008_T
2014_B
2014_L
2014_T
2018_B
2018_L
2018_T
2022_B
2022_L
2022_M
2022_T

D)

Figure 5: PCA All Samples

Plot of principal components (PC) 1 and 2 for all samples: A) Samples and ellipses color-coded by individual (KK number). B) Samples and ellipses color-coded by tissue type: B = bone, L = liver, M = muscle, T = toe pads C) Samples and ellipses color-coded by sex. D) Samples and ellipses color-coded by year. E) Samples with ellipses color-coded by germ layers. F) Samples with ellipses color-coded by internal organs. B = bone, I= internal organs (muscle and liver), and T = toe pads G) Samples and ellipses color-coded by county. H) Samples and ellipses color coded by KK number and symbols as tissue type. I) Samples and ellipses color-coded by KK number and symbols as year.

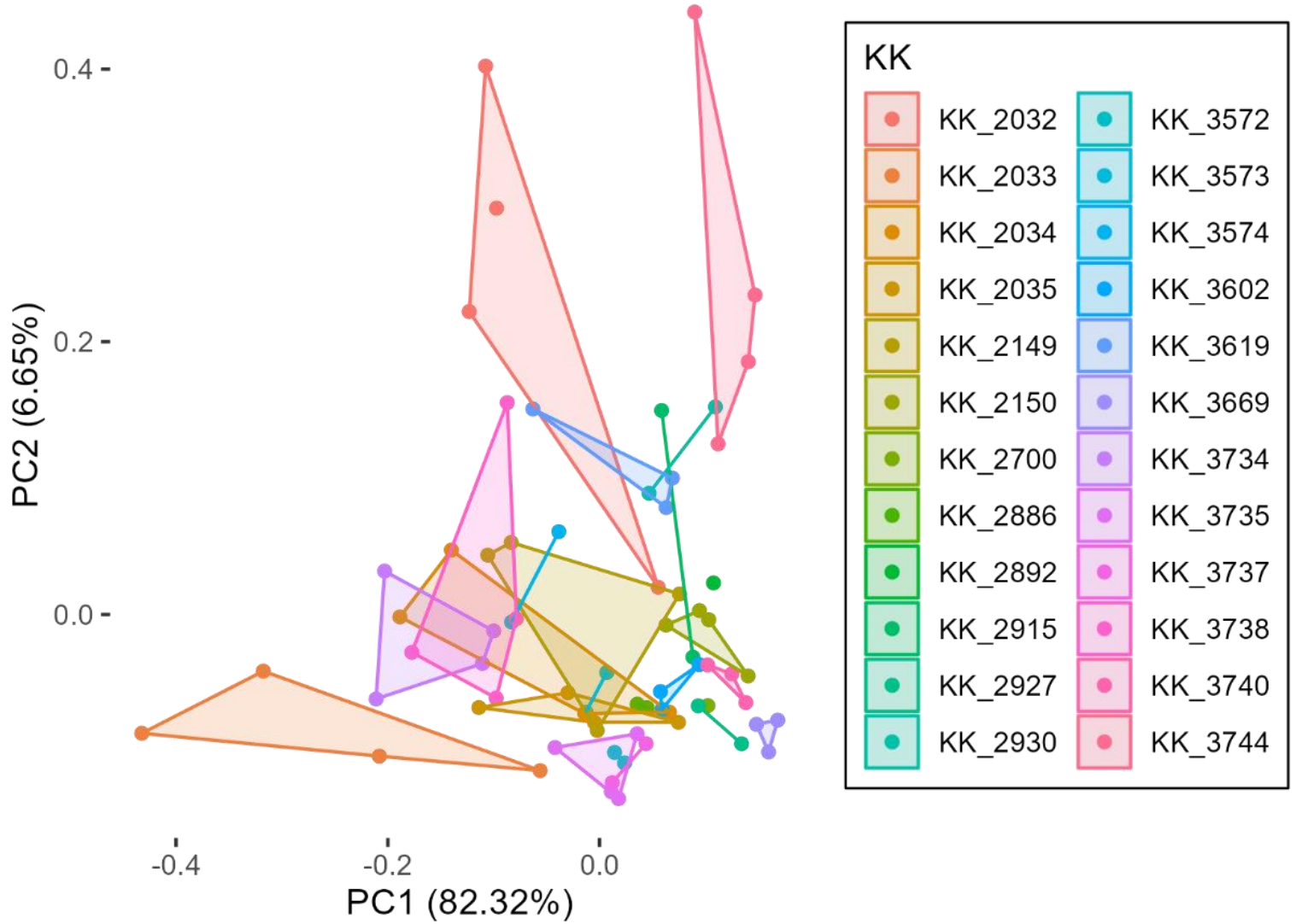
0.4
0.2
0.0
PC2 (6.65%)
-0.4
-0.2
0.0
PC1 (82.32%)
KK
KK_2032
KK_2033
KK_2034
KK_2035
KK_2149
KK_2150
KK_2700
KK_2886
KK_2892
KK_2915
KK_2927
KK_2930
KK_3572
KK_3573
KK_3574
KK_3602
KK_3619
KK_3669
KK_3734
KK_3735
KK_3737
KK_3738
KK_3740
KK_3744

A)

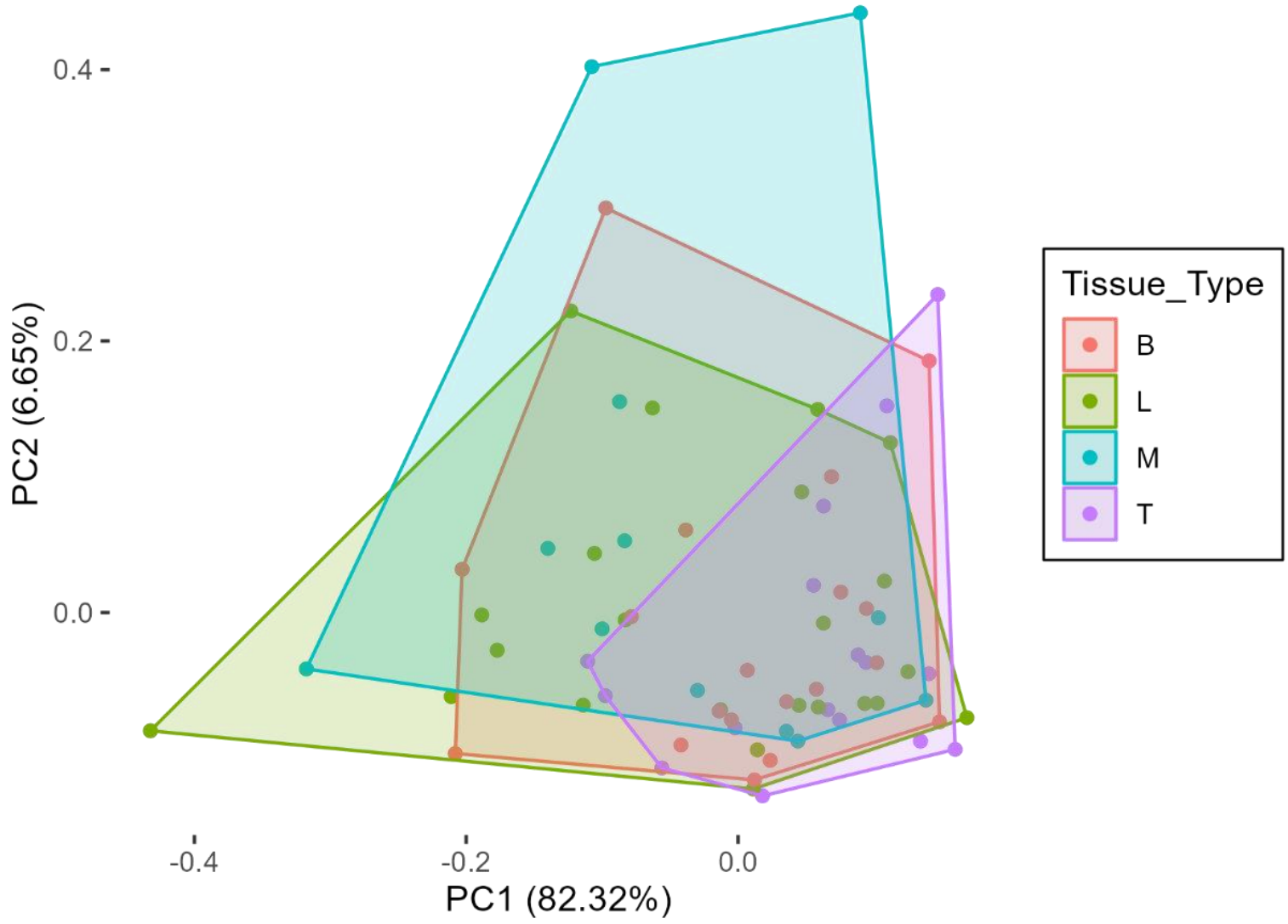

B)

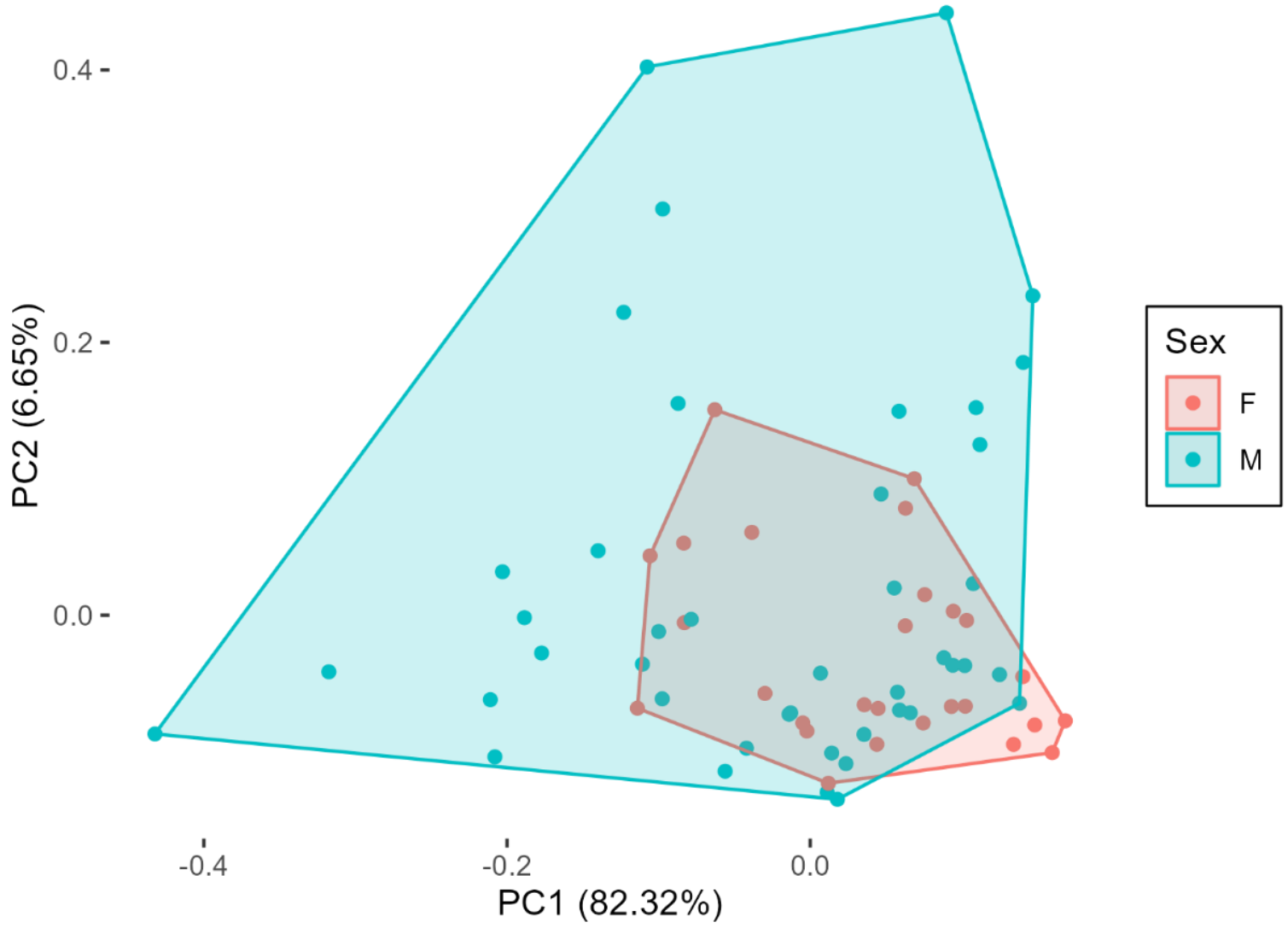

C)

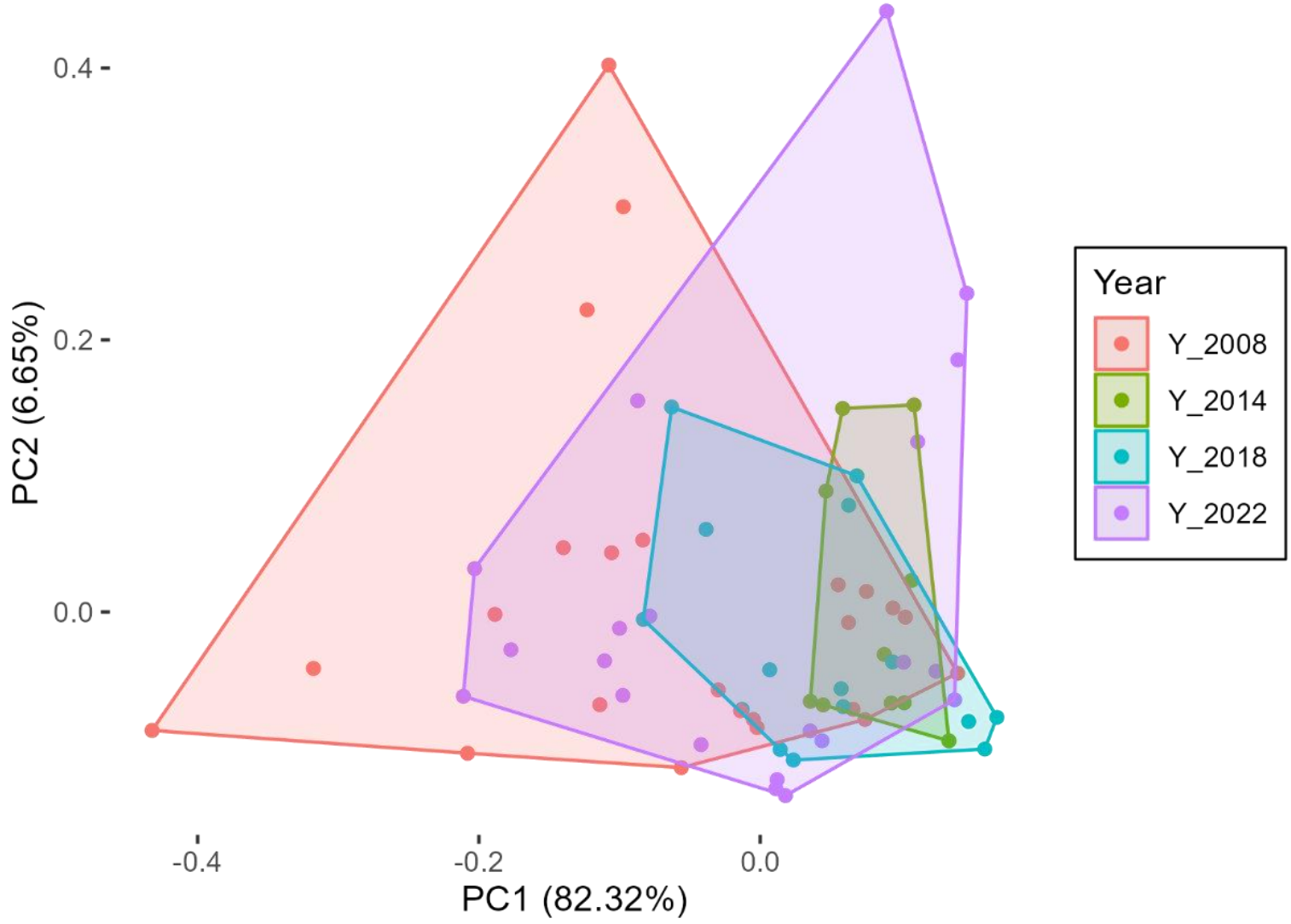

D)

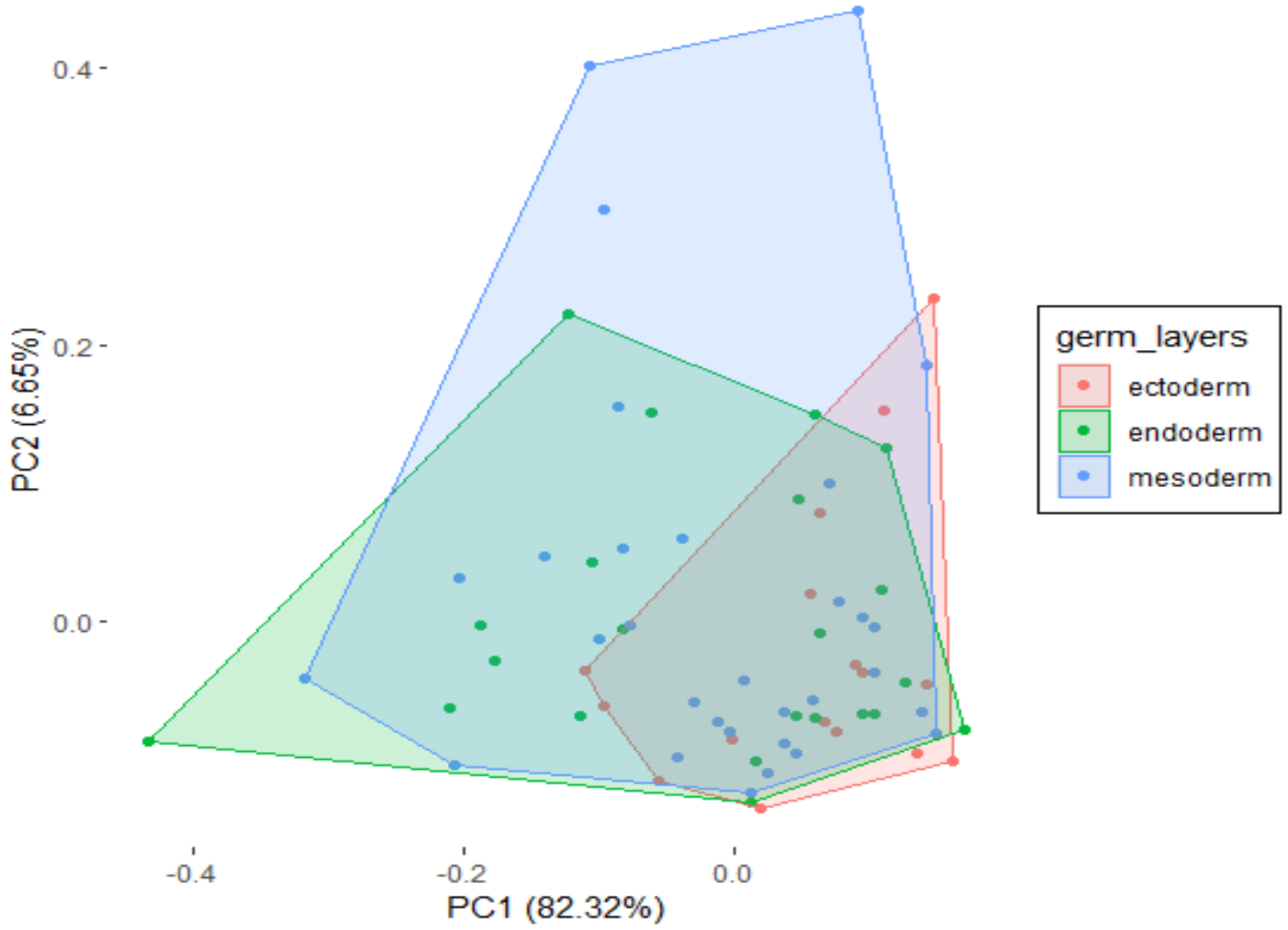
0.4
0.2
0.0
PC2 (6.65%)
-0.4
-0.2
0.0
PC1 (82.32%)
germ_layers
ectoderm
endoderm
mesoderm

E)

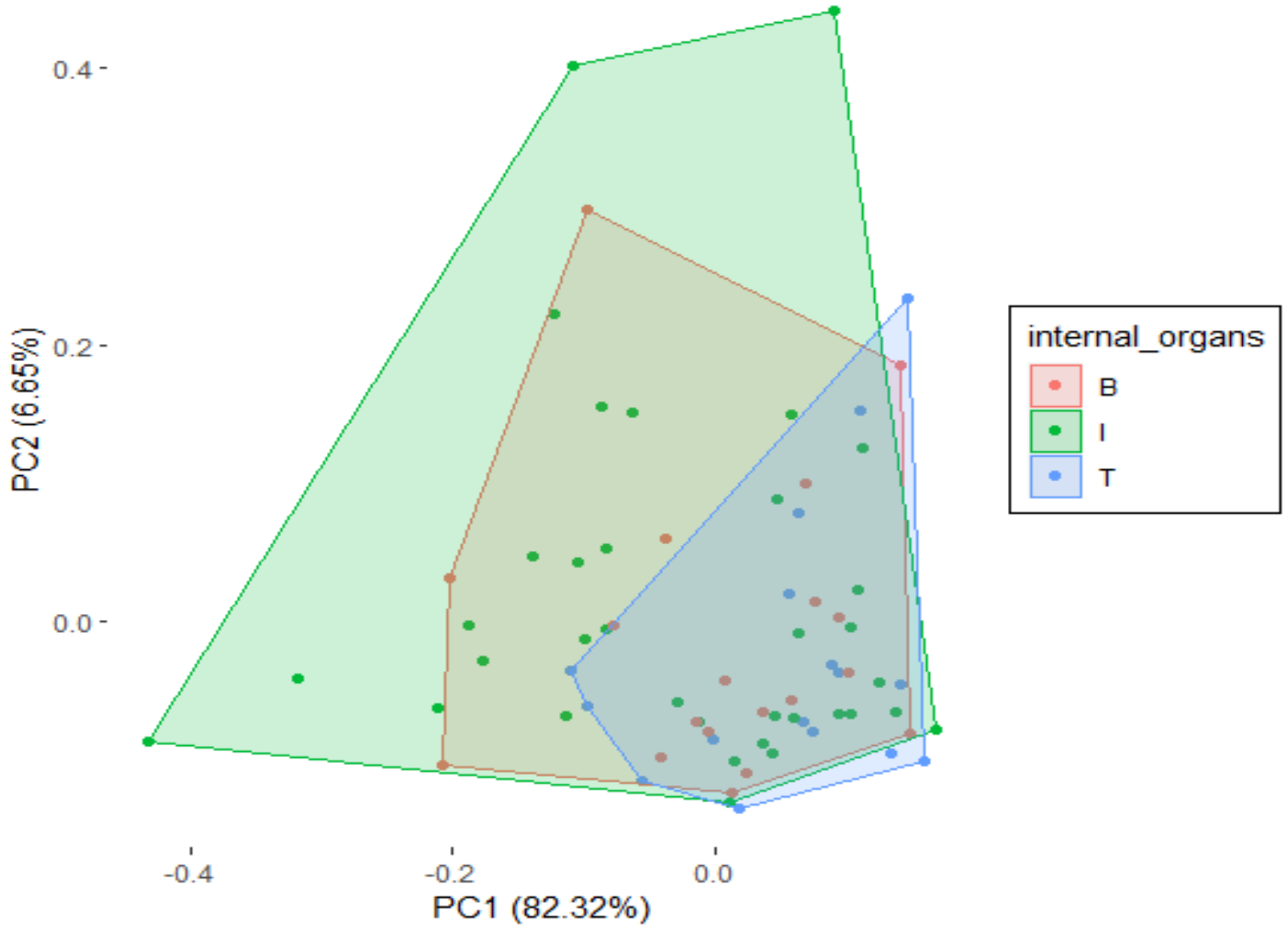

F)

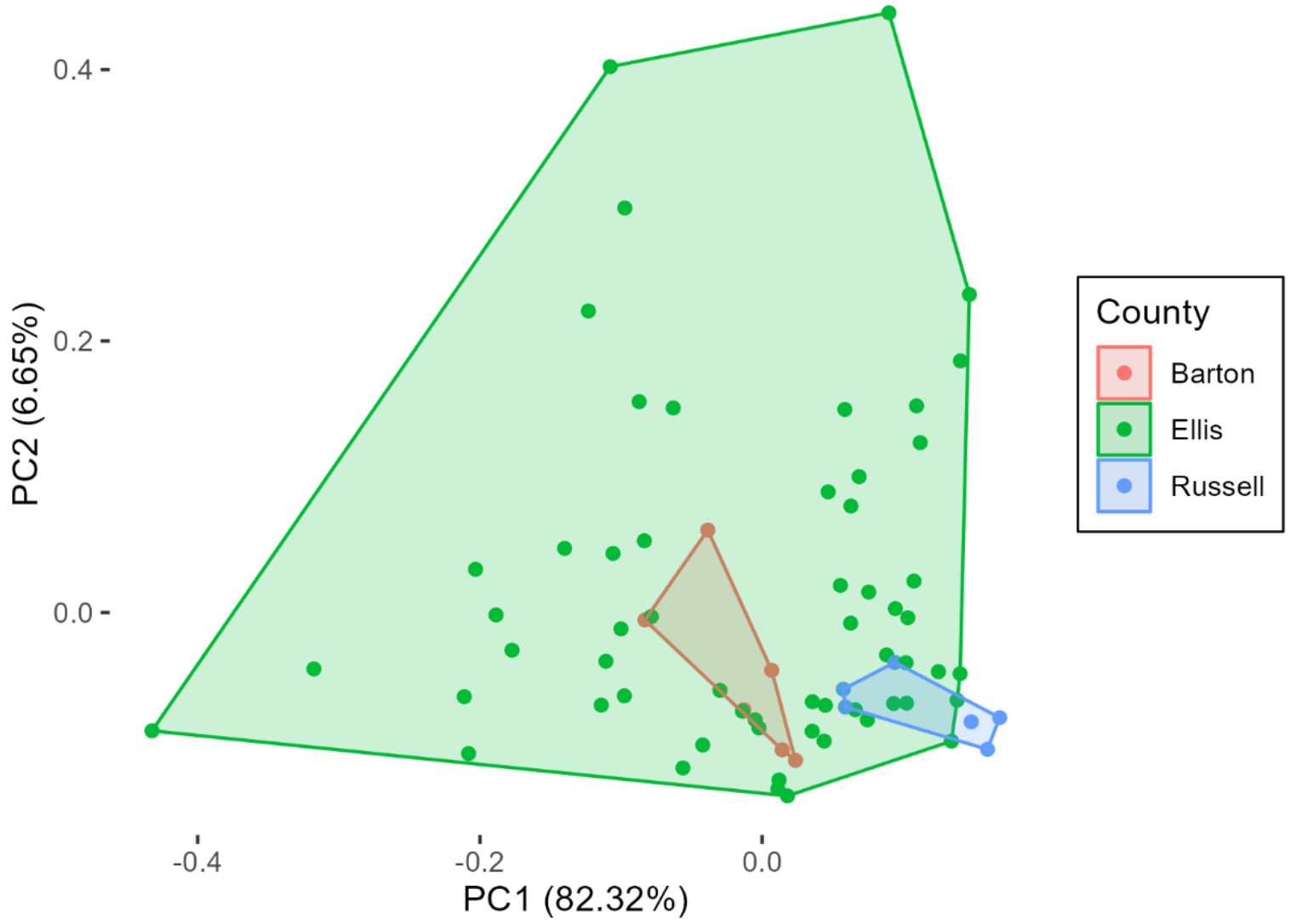

G)

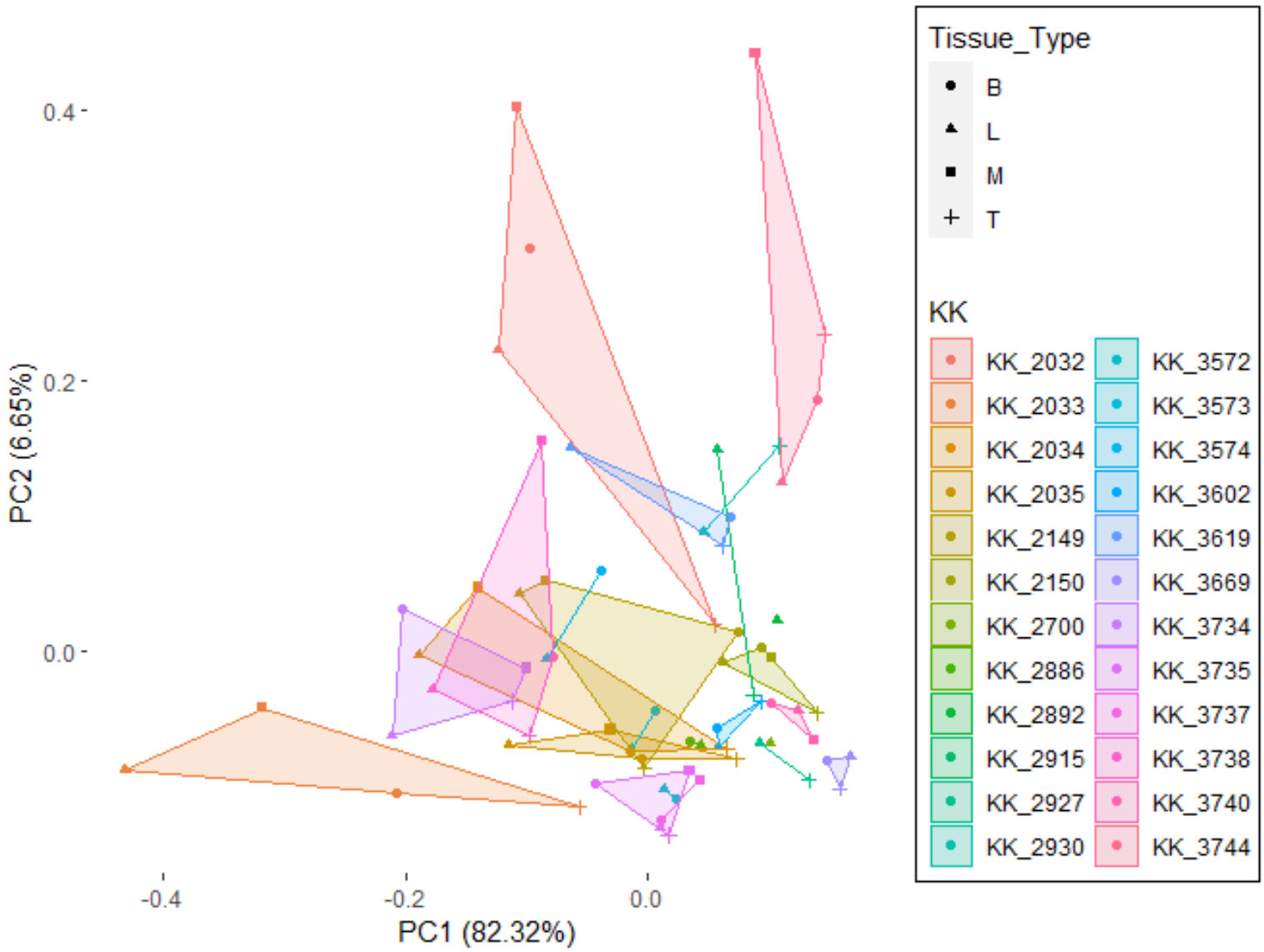
Tissue_Type
B
L
M
T
KK
KK_2032
KK_2033
KK_2034
KK_2035
KK_2149
KK_2150
KK_2700
KK_2886
KK_2892
KK_2915
KK_2927
KK_2930
KK_3572
KK_3573
KK_3574
KK_3602
KK_3619
KK_3669
KK_3734
KK_3735
KK_3737
KK_3738
KK_3740
KK_3744
0.4
0.2
0.0
PC2 (6.65%)
-0.4
-0.2
0.0
PC1 (82.32%)

H)

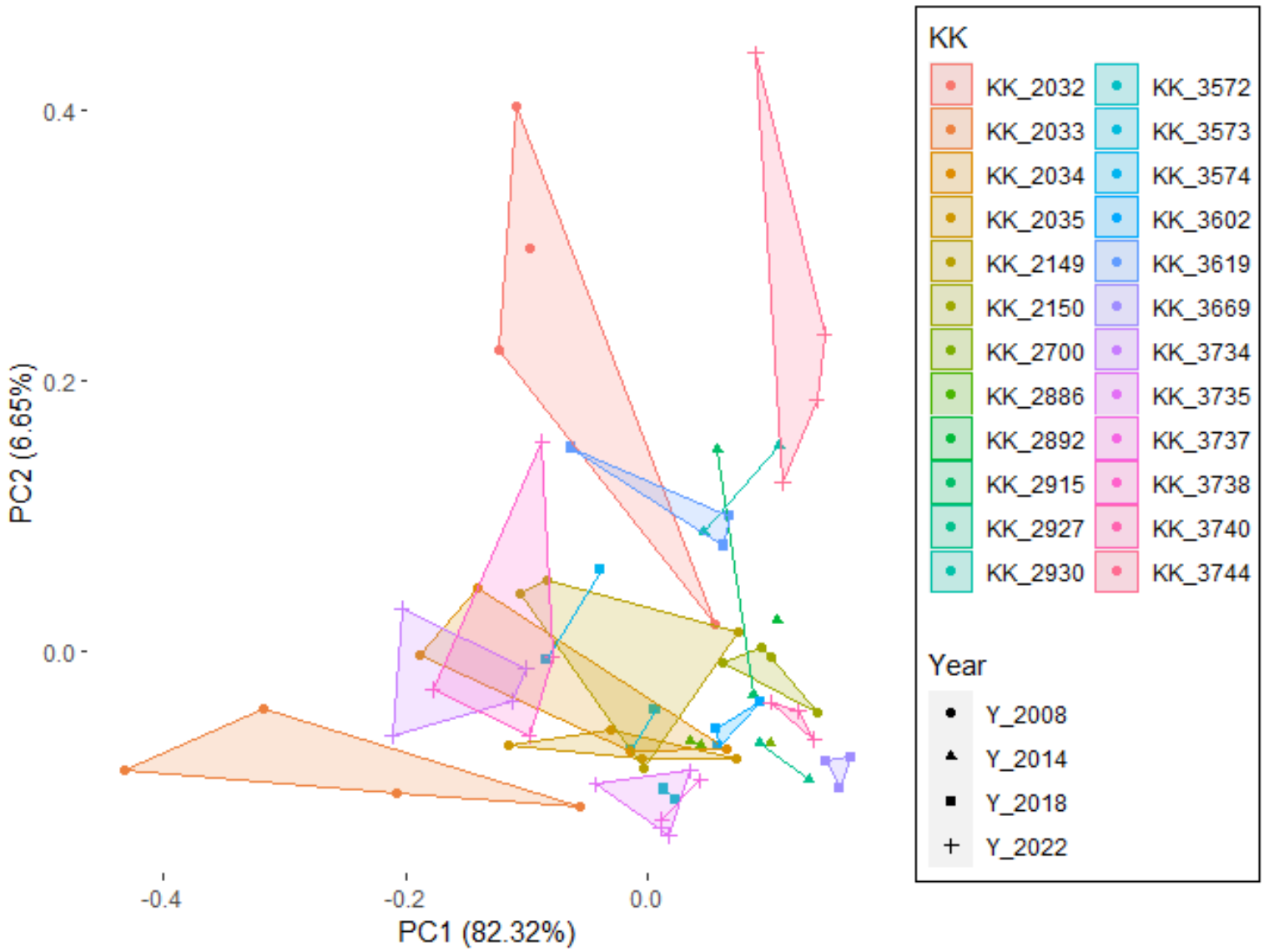
0.4
0.2
0.0
PC2 (6.65%)
-0.4
-0.2
0.0
PC1 (82.32%)
KK
KK_2032
KK_2033
KK_2034
KK_2035
KK_2149
KK_2150
KK_2700
KK_2886
KK_2892
KK_2915
KK_2927
KK_2930
KK_3572
KK_3573
KK_3574
KK_3602
KK_3619
KK_3669
KK_3734
KK_3735
KK_3737
KK_3738
KK_3740
KK_3744
Year
Y_2008
Y_2014
Y_2018
Y_2022

I)

Figure 6: PCA 2022

Plot of principal components (PC) 1 and 2 for samples collected in 2022: A) Samples and ellipses color-coded by KK number. B) Samples and ellipses color-coded by tissue type: B = bone, L = liver, M = muscle, T = toe pads C) Samples and ellipses color-coded by sex. D) Samples and ellipses color-coded by county.

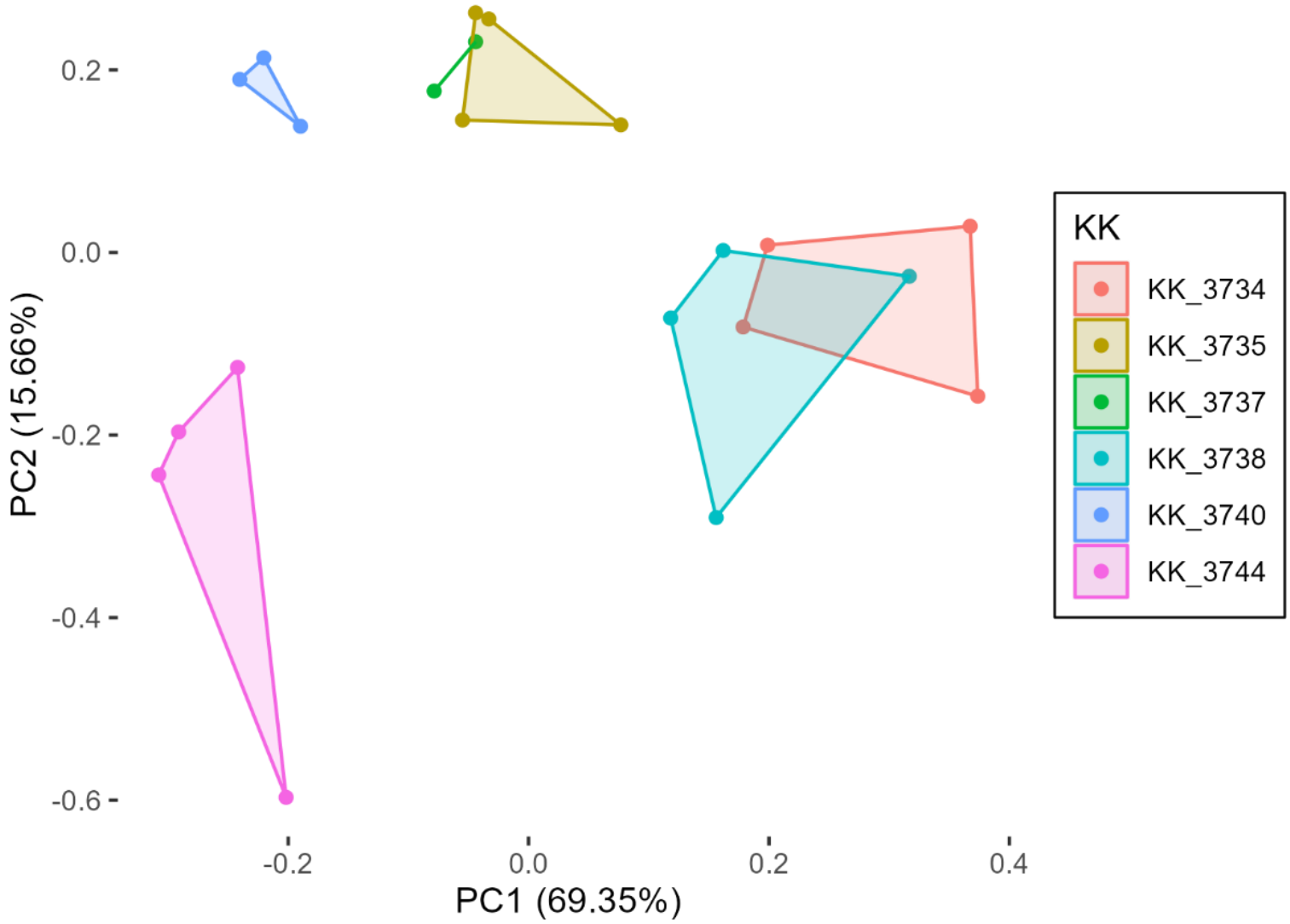
0.2
0.0
-0.2
-0.4
-0.6
PC2 (15.66%)
-0.2
0.0
0.2
0.4
PC1 (69.35%)
KK
KK_3734
KK_3735
KK_3737
KK_3738
KK_3740
KK_3744

A)

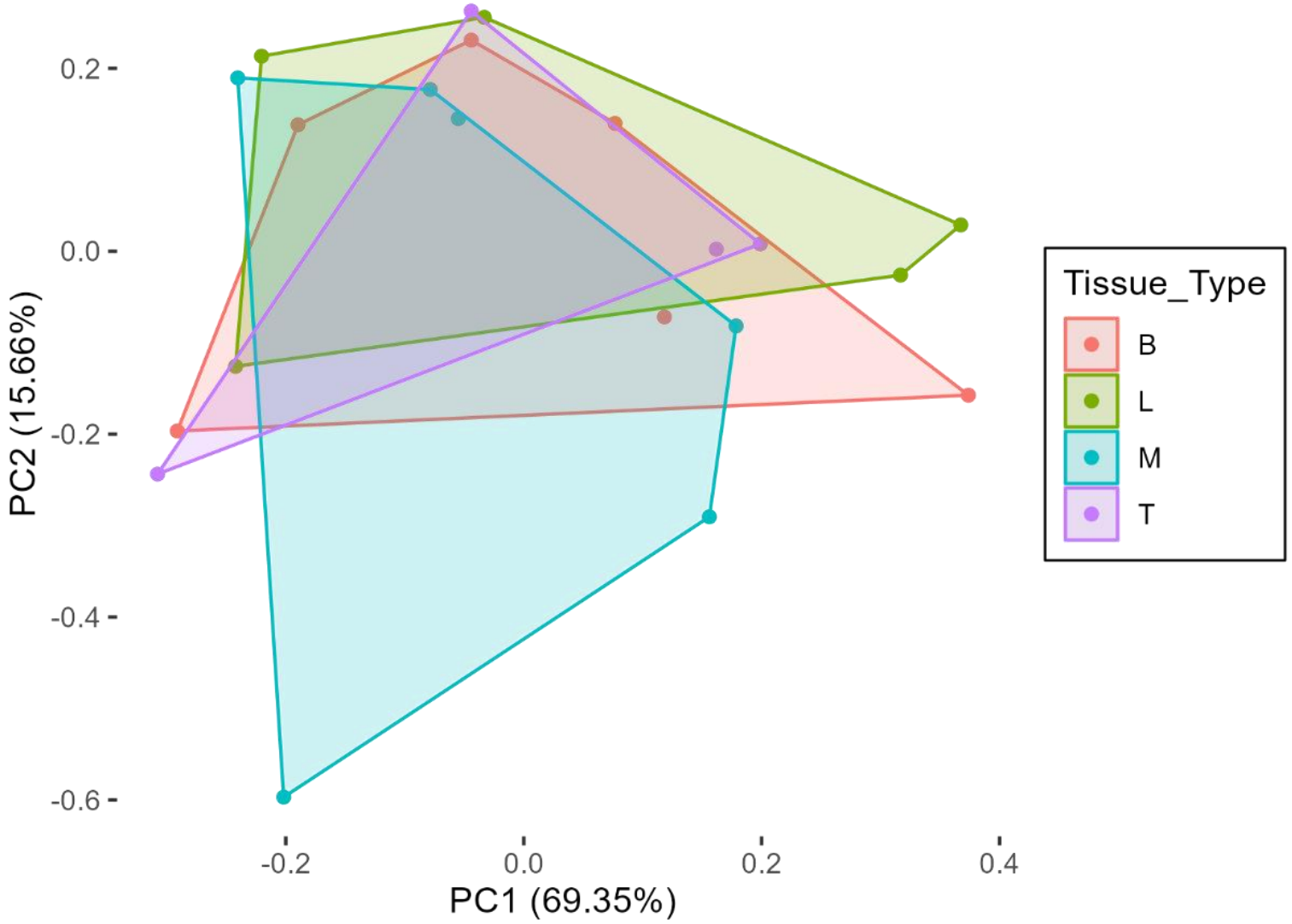

B)

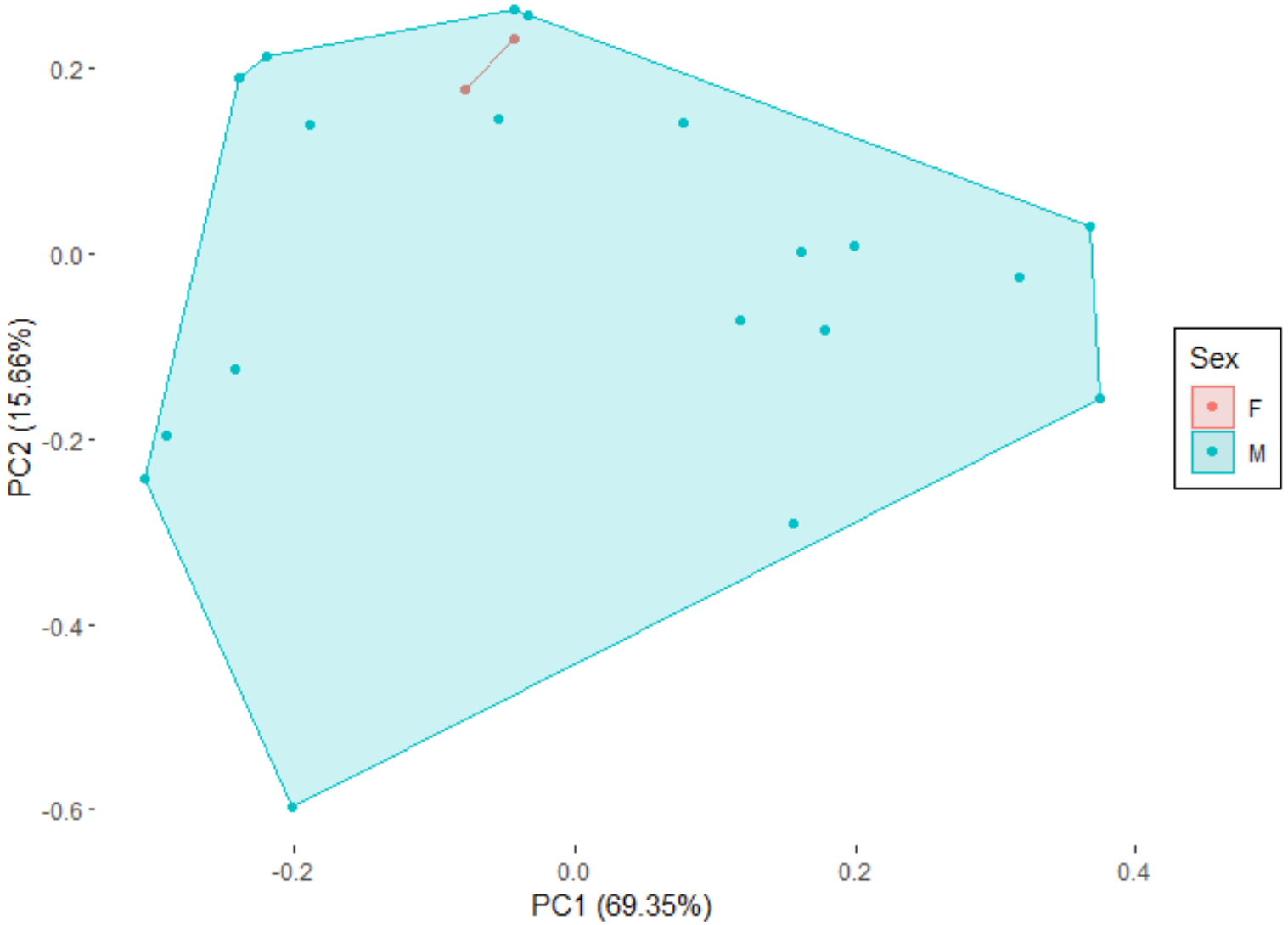

C)

Figure 7: PCA 2018

Plot of principal component (PC) 1 and 2 for samples collected in 2018: A) Samples and ellipses color-coded by KK number. B) Samples and ellipses color-coded by tissue type: B = bone, L = liver, T = toe pads C) Samples and ellipses color-coded by sex. D) Samples and ellipses color-coded by county.

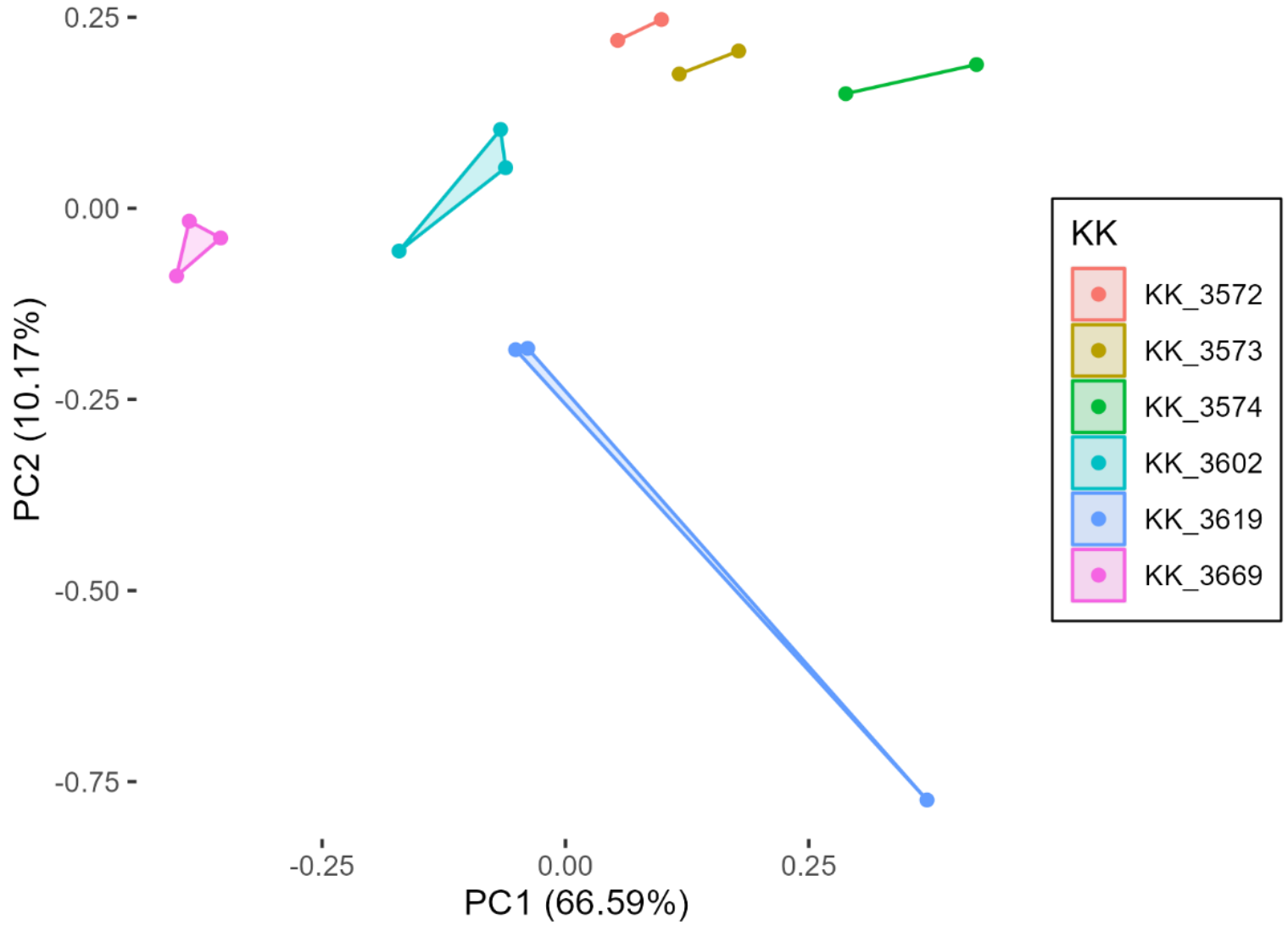
0.25
0.00
-0.25
-0.50
-0.75
PC2 (10.17%)
-0.25
0.00
0.25
PC1 (66.59%)
KK
KK_3572
KK_3573
KK_3574
KK_3602
KK_3619
KK_3669

A)

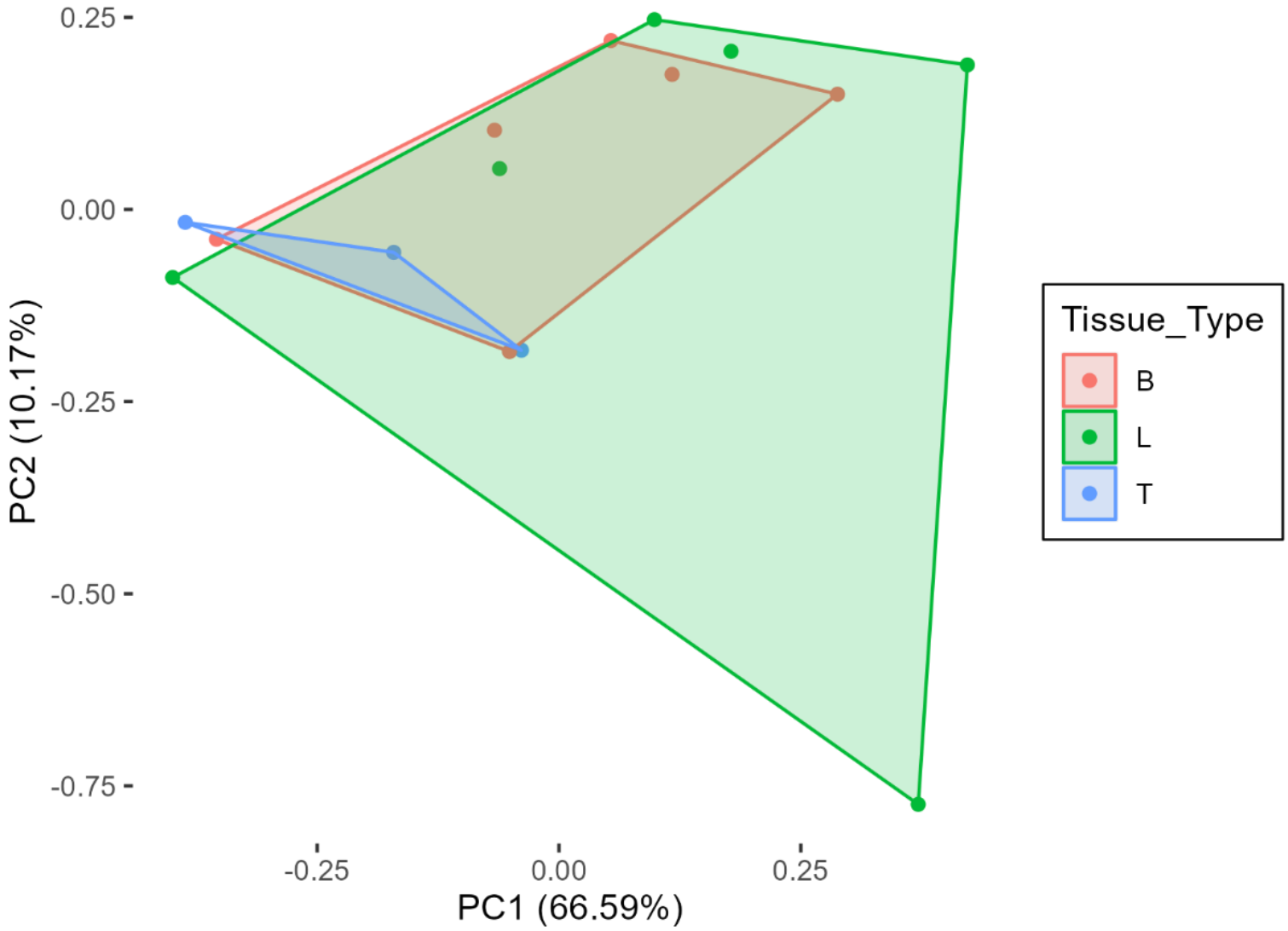
0.25
0.00
-0.25
-0.50
-0.75
PC2 (10.17%)
-0.25
0.00
0.25
PC1 (66.59%)
Tissue_Type
B
L
T

B)

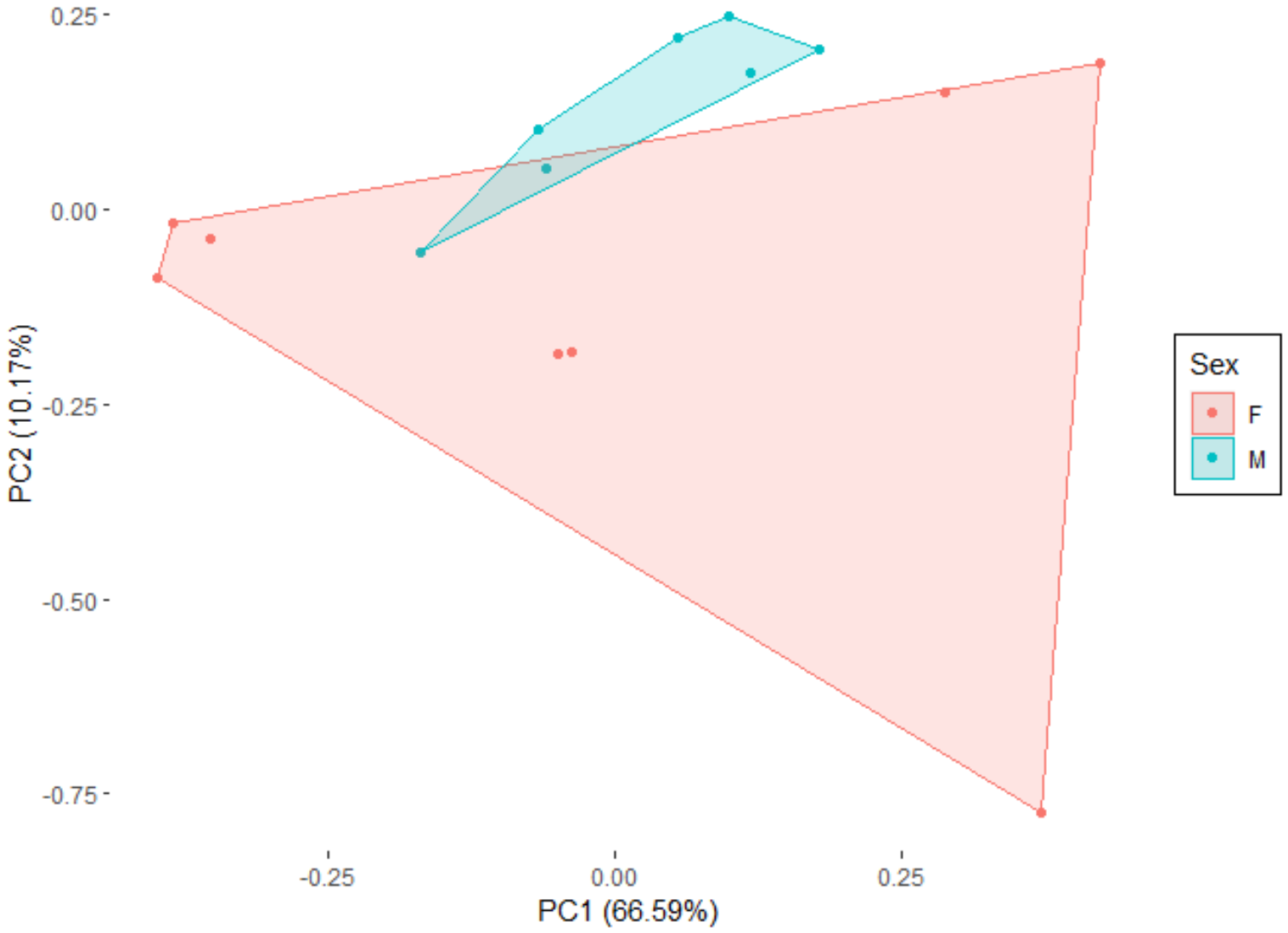

C)

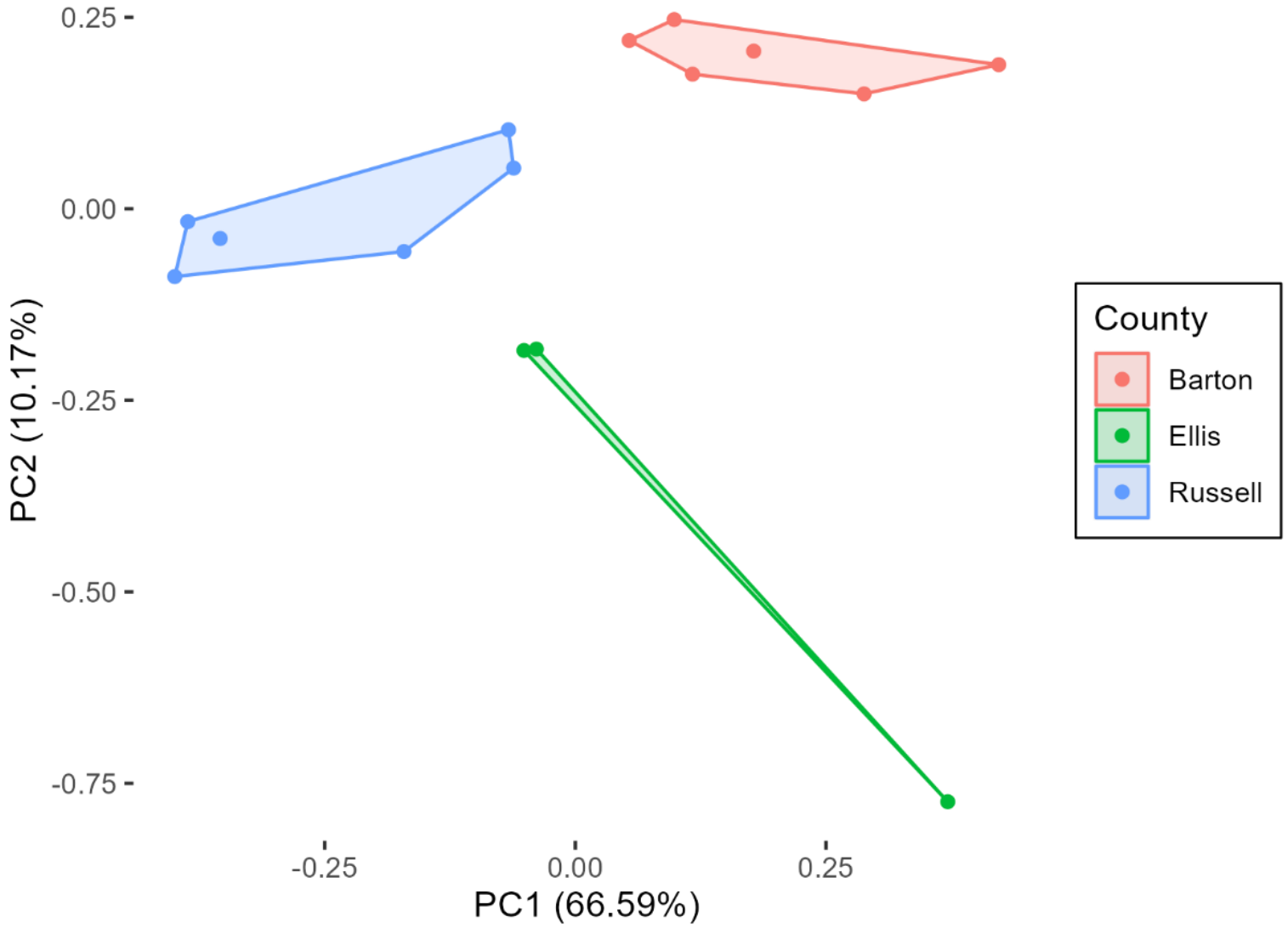
0.25
0.00
-0.25
-0.50
-0.75
PC2 (10.17%)
-0.25
0.00
0.25
PC1 (66.59%)
County
Barton
Ellis
Russell

D)

Figure 8: PCA 2014

Plot of principal component (PC) 1 and 2 from samples collected in 2014: A) Samples and ellipses color-coded by KK number. B) Samples and ellipses color-coded by tissue type: B = bone, L = liver, T = toe pads C) Samples and ellipses color-coded by sex.

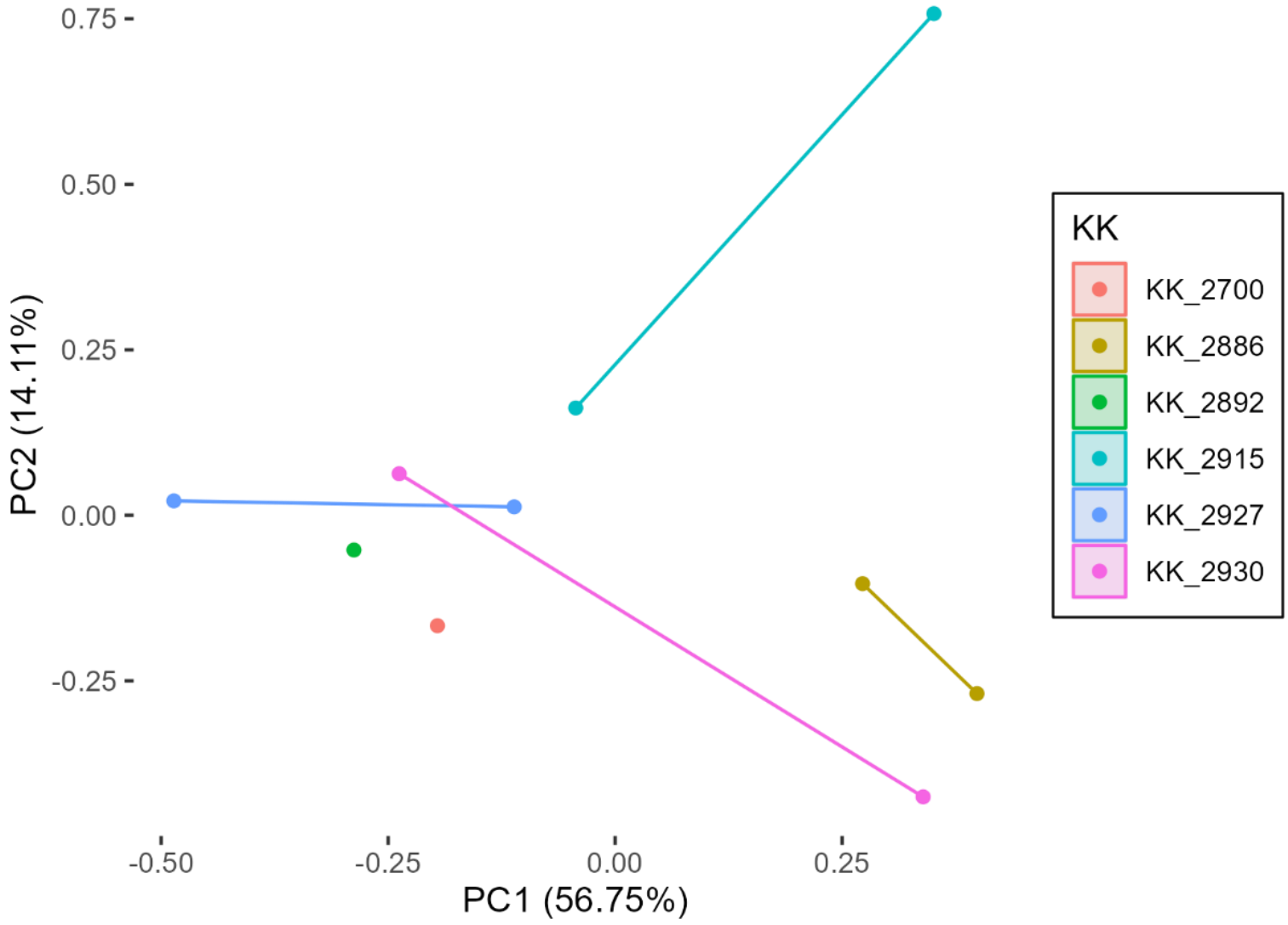
0.75
0.50
0.25
0.00
-0.25
PC2 (14.11%)
-0.50
-0.25
0.00
0.25
PC1 (56.75%)
KK
KK_2700
KK_2886
KK_2892
KK_2915
KK_2927
KK_2930

A)

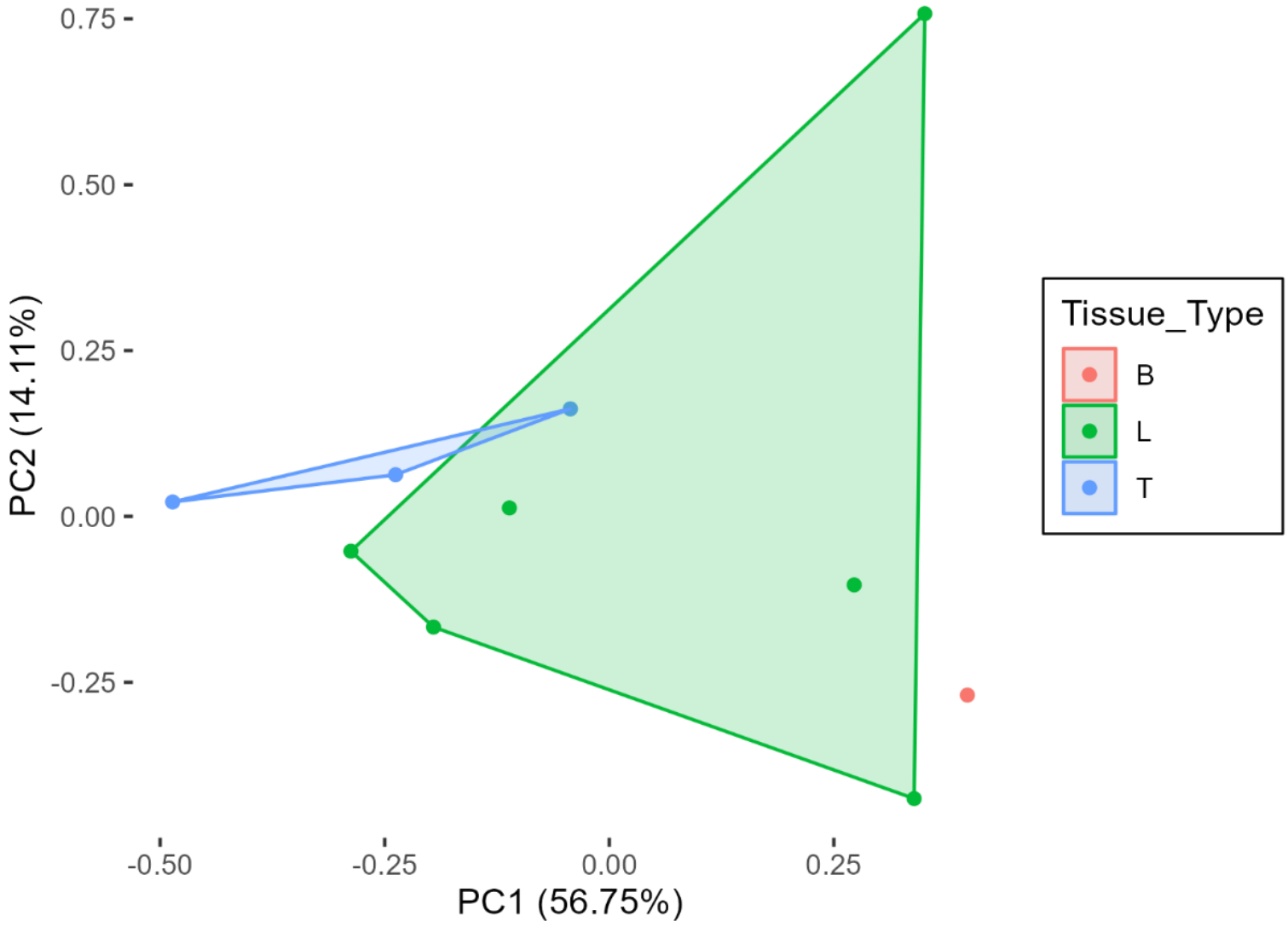
0.75
0.50
0.25
0.00
-0.25
PC2 (14.11%)
-0.50
-0.25
0.00
0.25
PC1 (56.75%)
Tissue_Type
B
L
T

B)

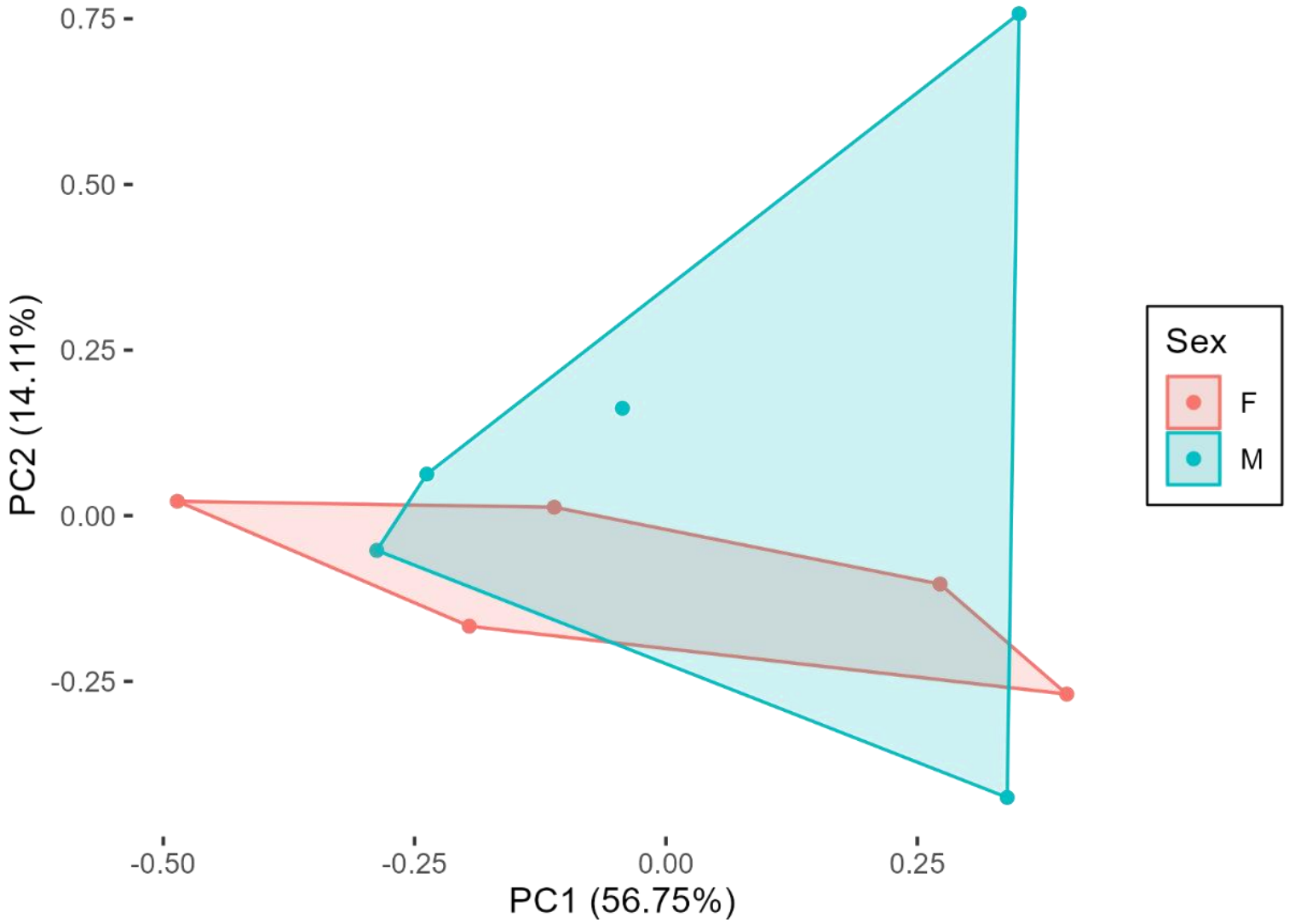

C)

Figure 9: PCA 2008

Plot of principal component (PC) 1 and 2 from samples collected in 2008: A) Samples and ellipses color-coded by KK number. B) Samples and ellipses color-coded by tissue type: B = bone, L = liver, M = muscle, T = toe pads C) Samples and ellipses color-coded by sex. D) Samples and ellipses color-coded by county.

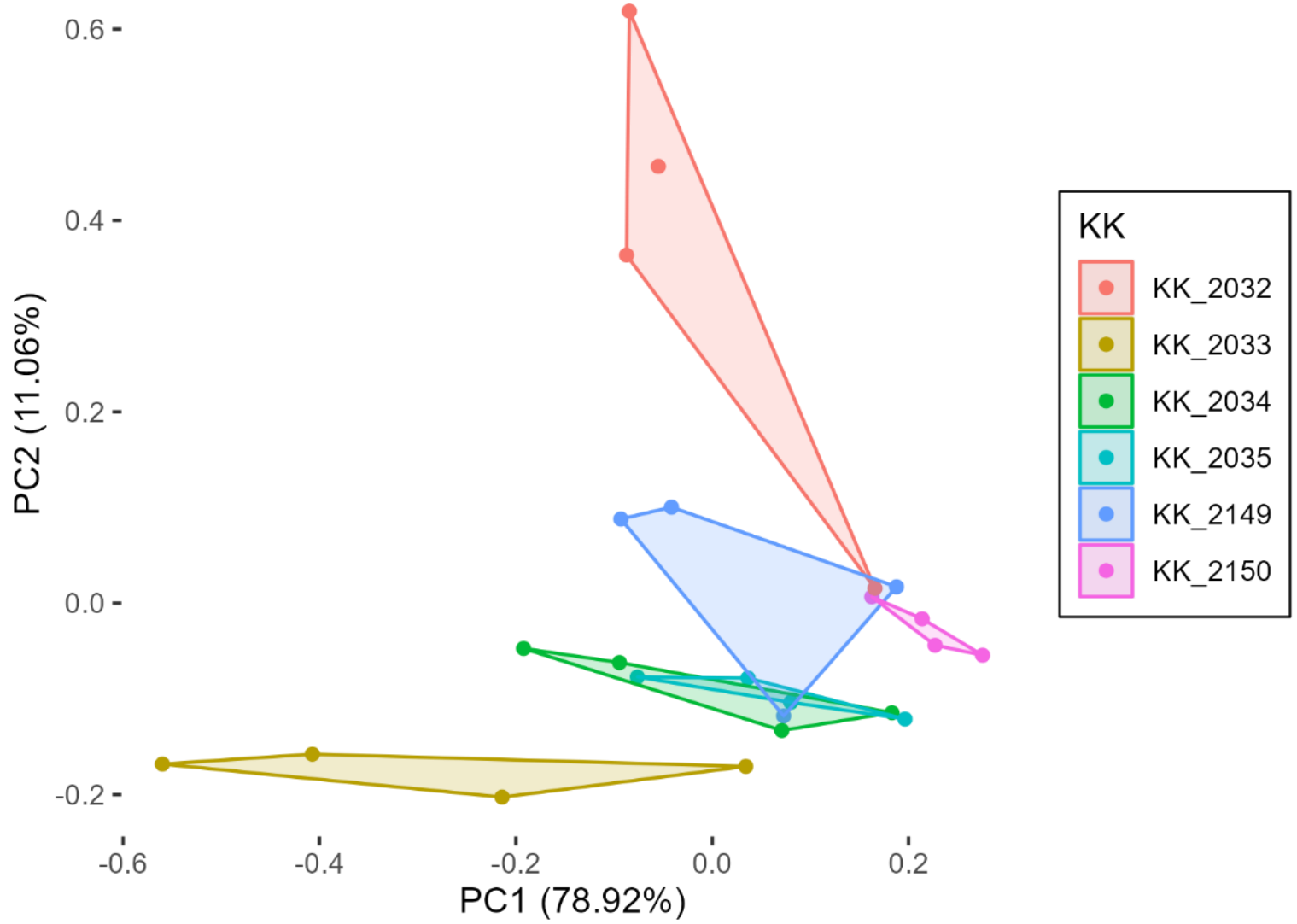
0.6
0.4
0.2
0.0
-0.2
PC2 (11.06%)
-0.6
-0.4
-0.2
0.0
0.2
PC1 (78.92%)
KK
KK_2032
KK_2033
KK_2034
KK_2035
KK_2149
KK_2150

A)

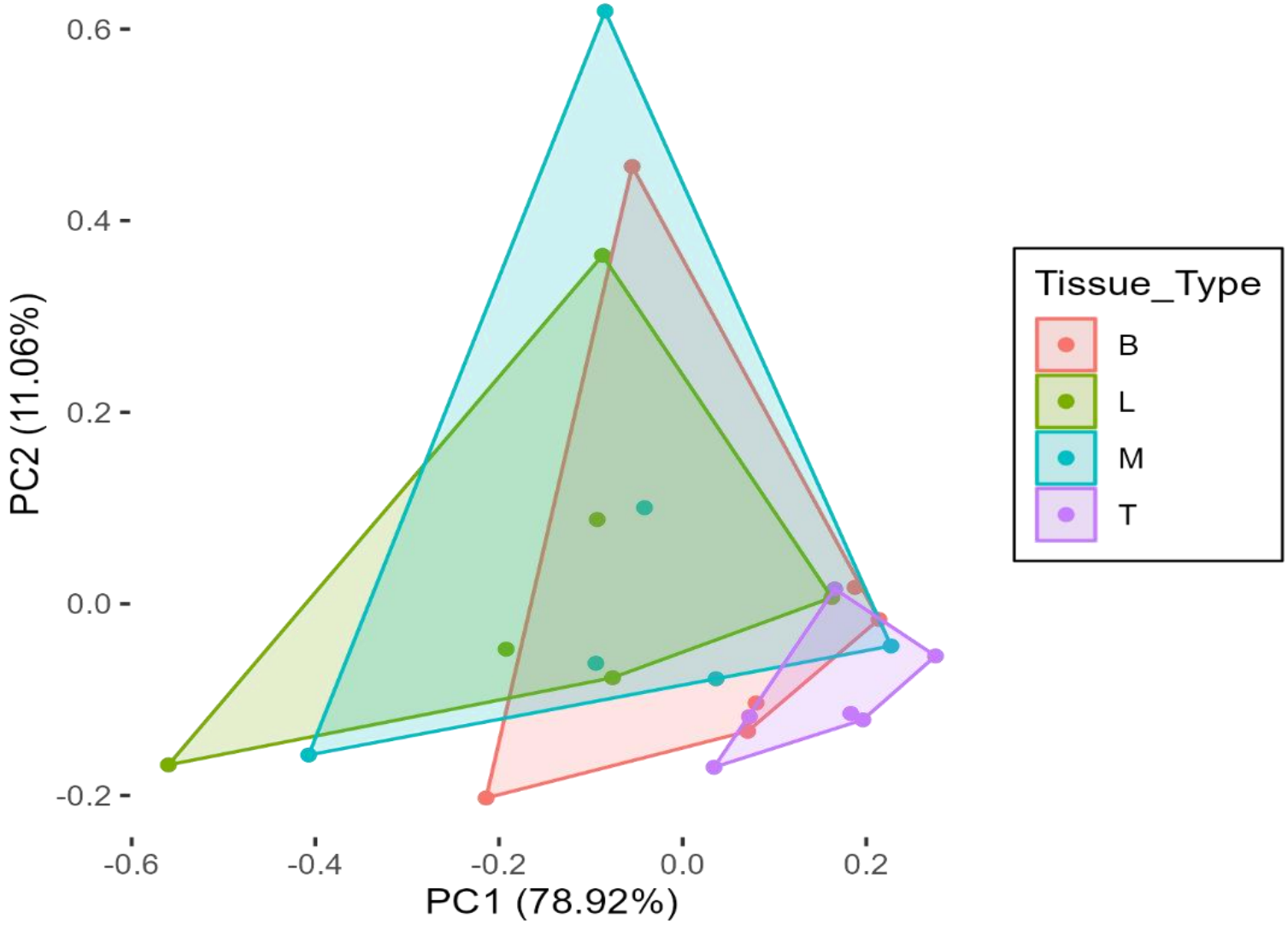

B)

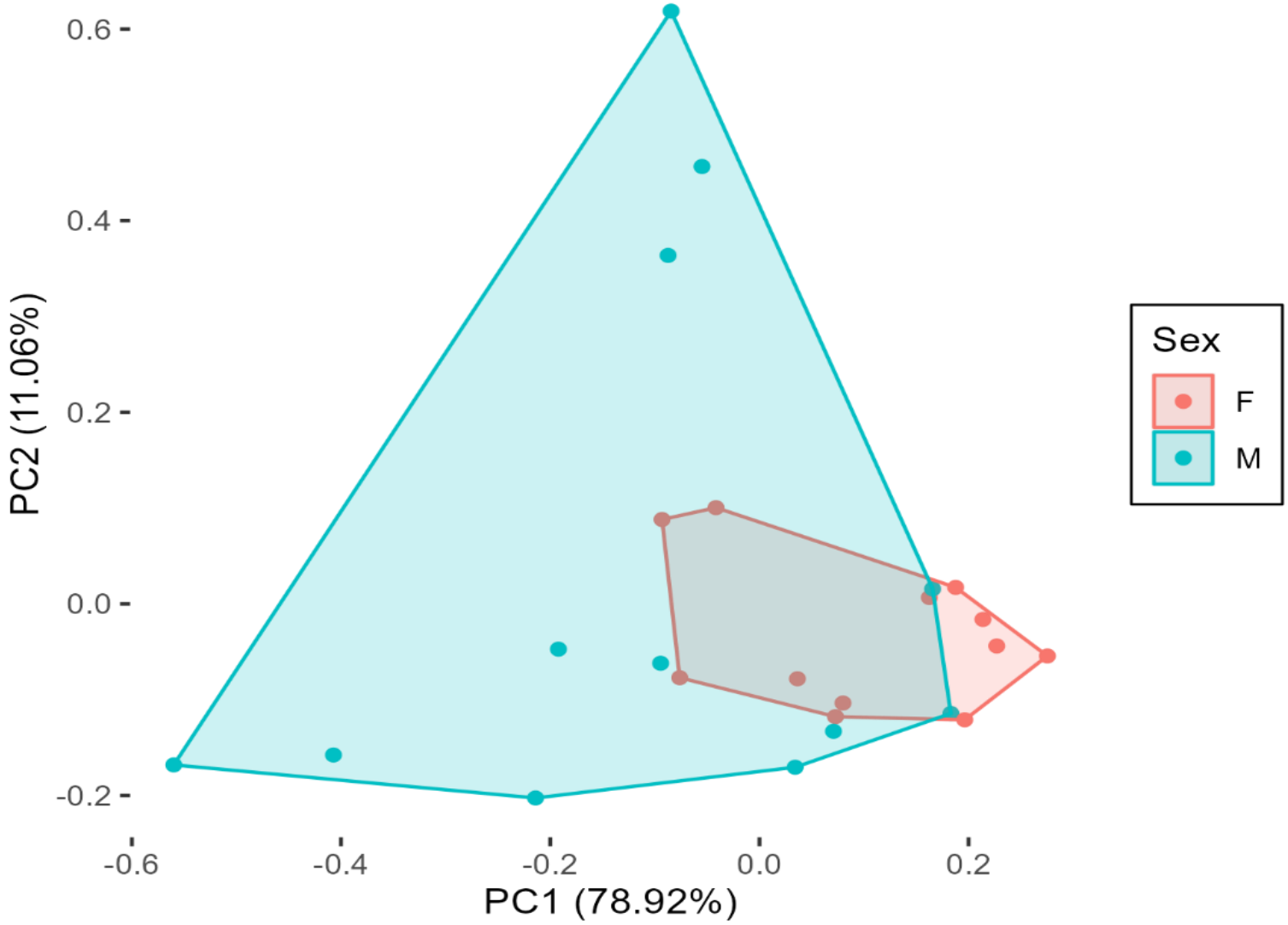

C)

Figure 10: PCA Ethanol vs No Ethanol

Plot of principal component (PC) 1 and 2 from samples collected in 2022 for ethanol versus no ethanol: A) Samples and ellipses color-coded by KK number. B) Samples and ellipses color-coded by tissue type: L = liver, M = muscle C) Samples and ellipses color-coded by sex. D) Samples and ellipses color-coded by ethanol or no ethanol.

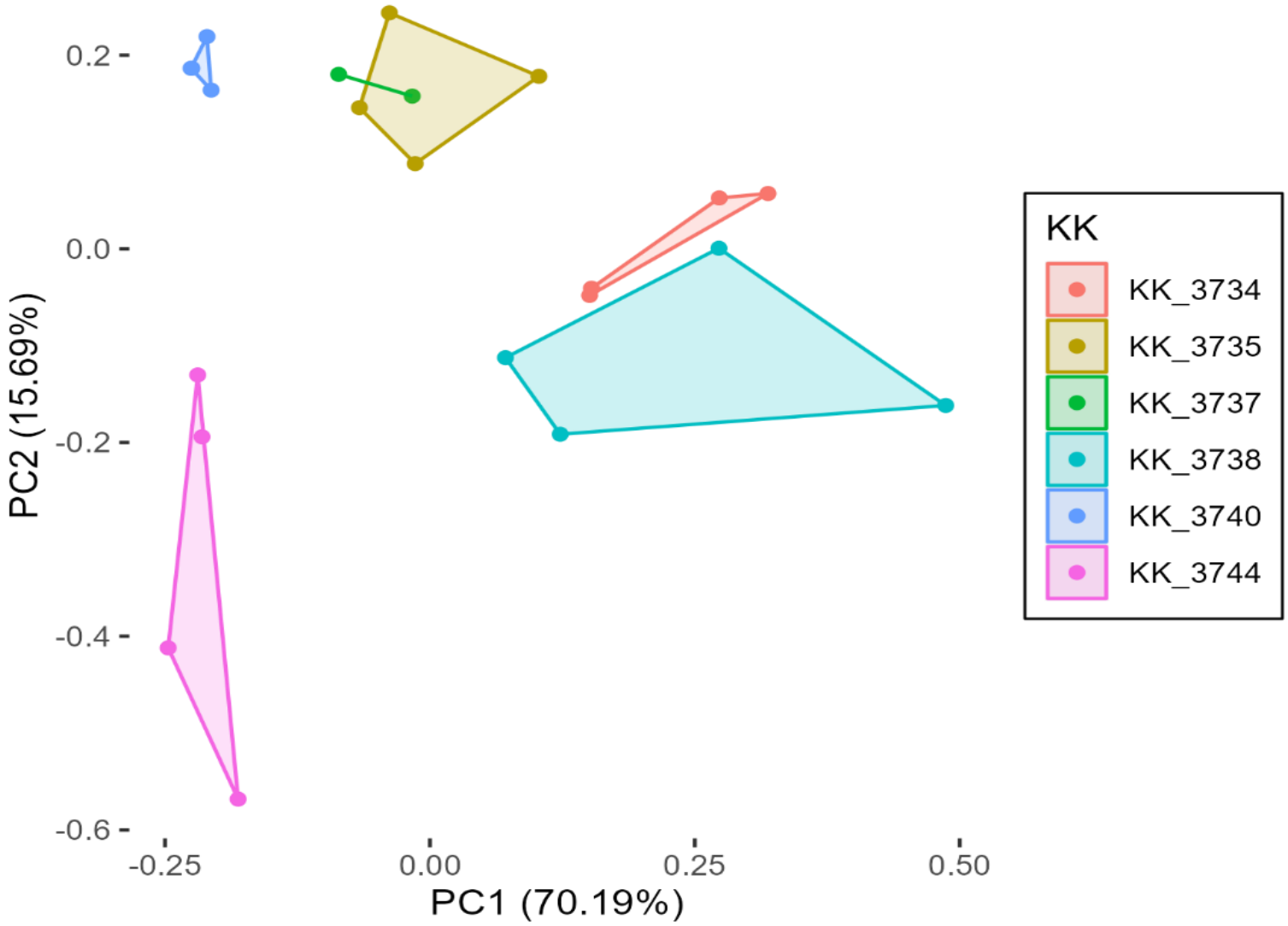
0.2
0.0
-0.2
-0.4
-0.6
PC2 (15.69%)
-0.25
0.00
0.25
0.50
PC1 (70.19%)
KK
KK_3734
KK_3735
KK_3737
KK_3738
KK_3740
KK_3744

A)

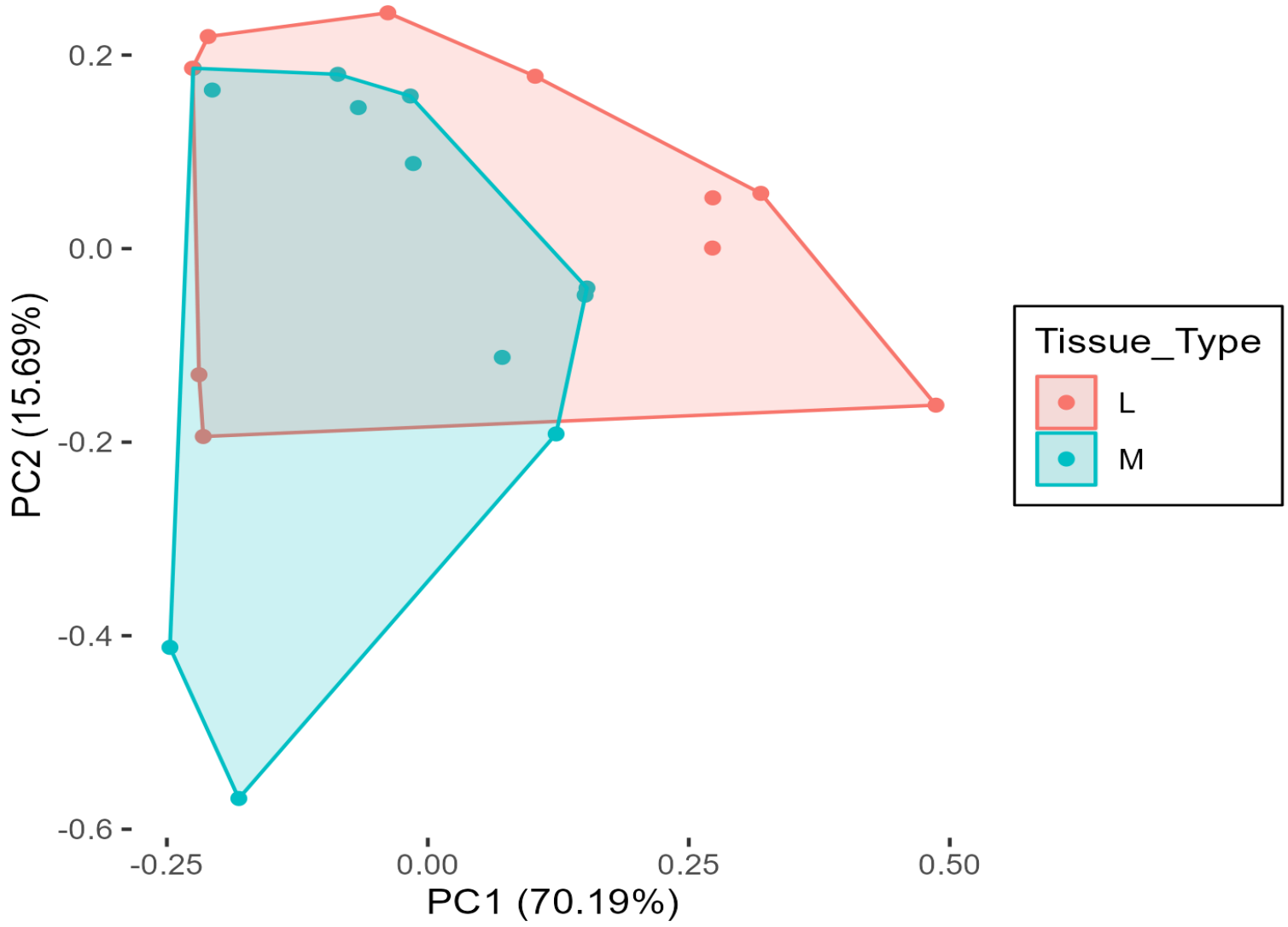

B)

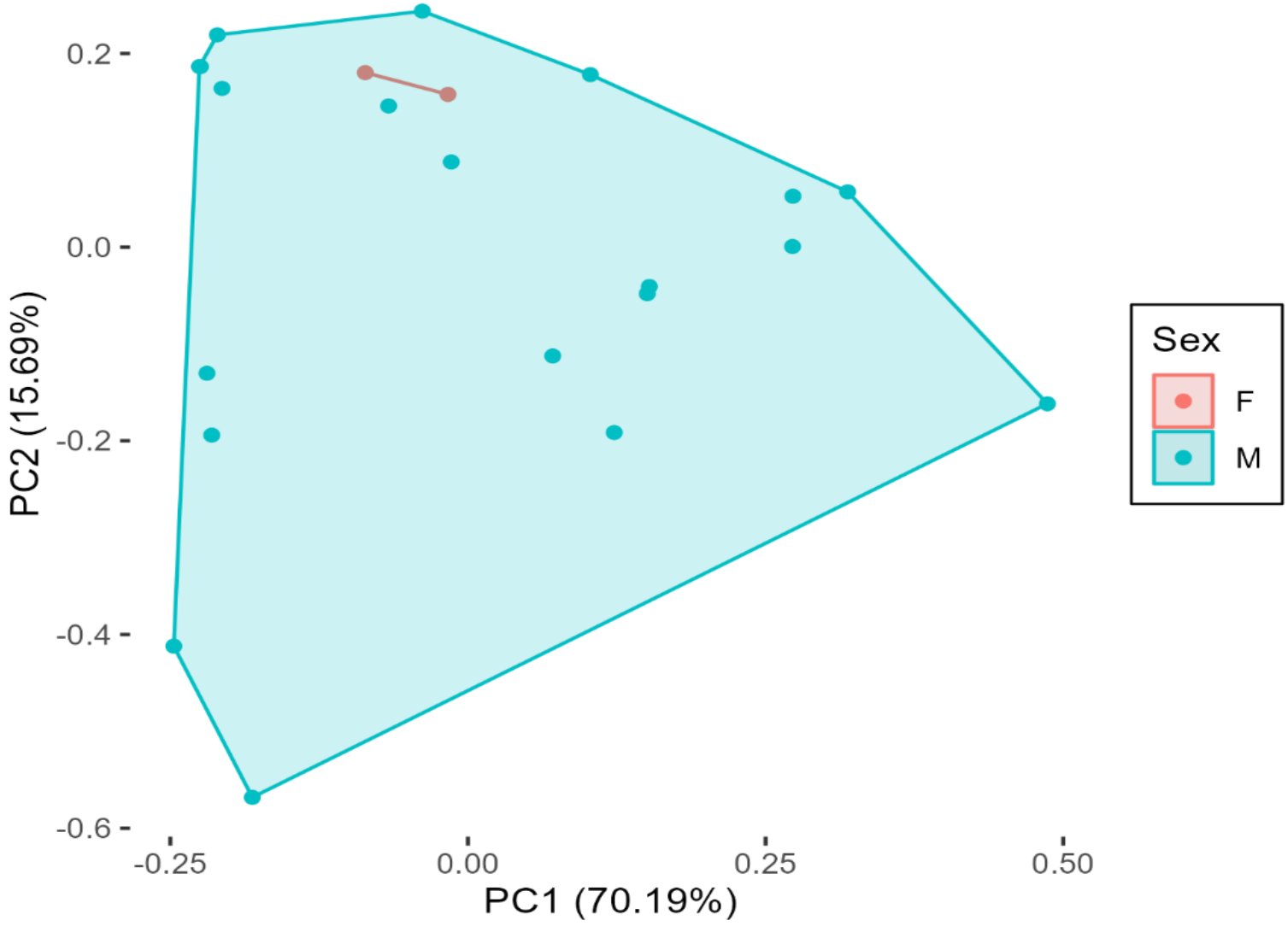

C)

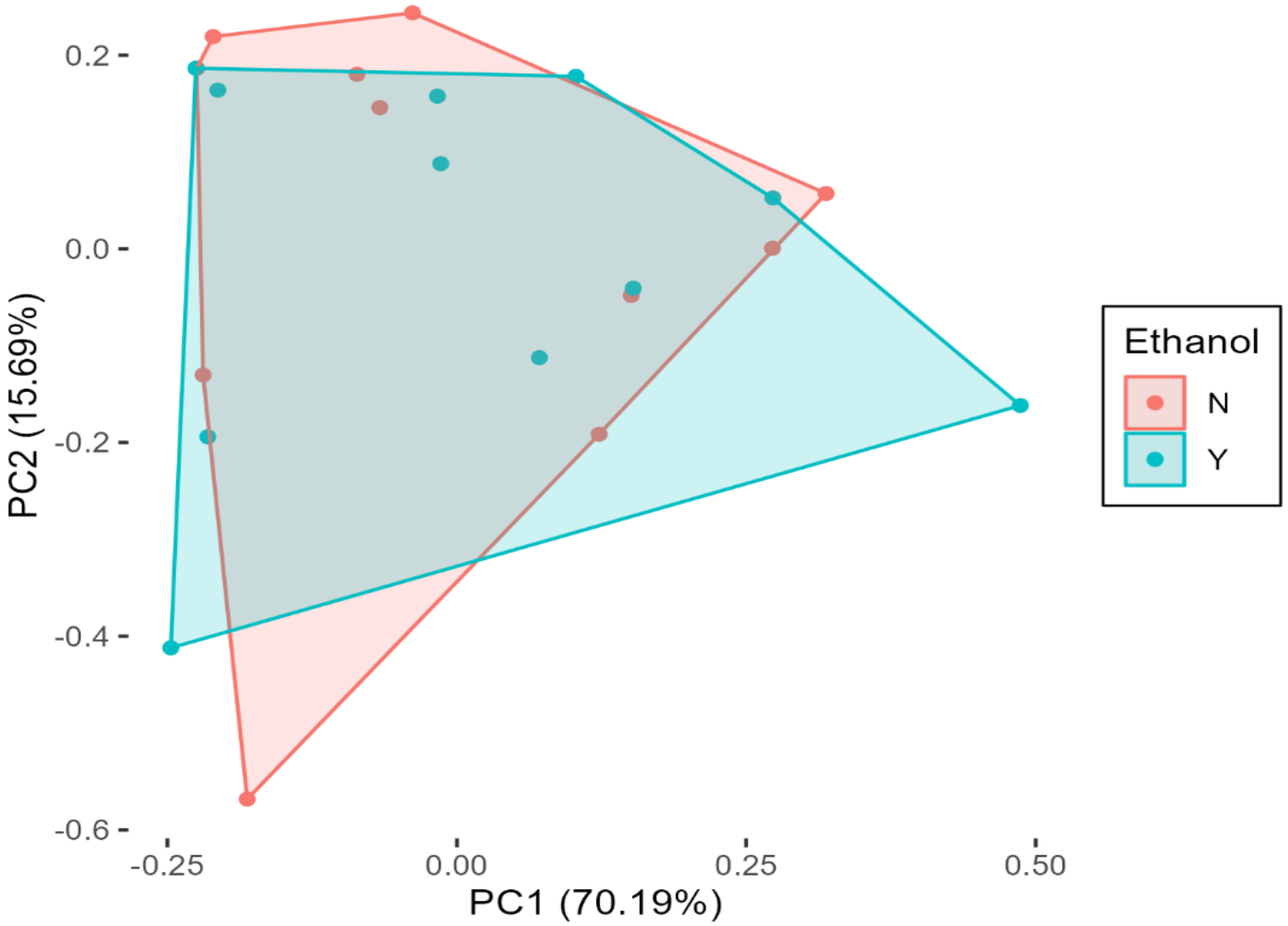

D)

Figure 11: Bar Plots

CpG percent Methylation and Total Percent Methylation. Liver with ethanol = L_E, liver without ethanol = L_NE, muscle with ethanol = M_E, muscle with no ethanol = M_NE A) CpG Percent Methylation B) Total Percent Methylation

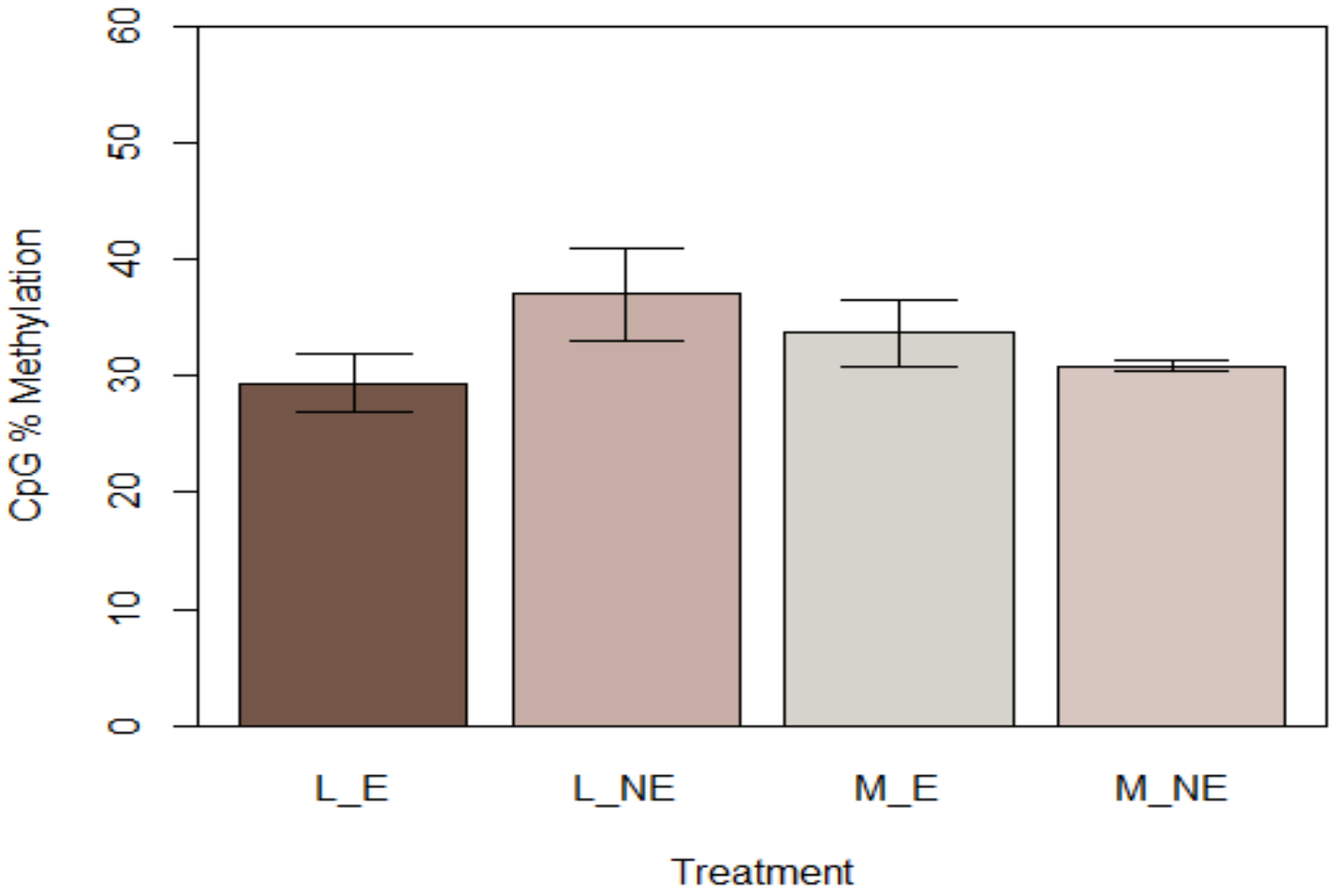

A)

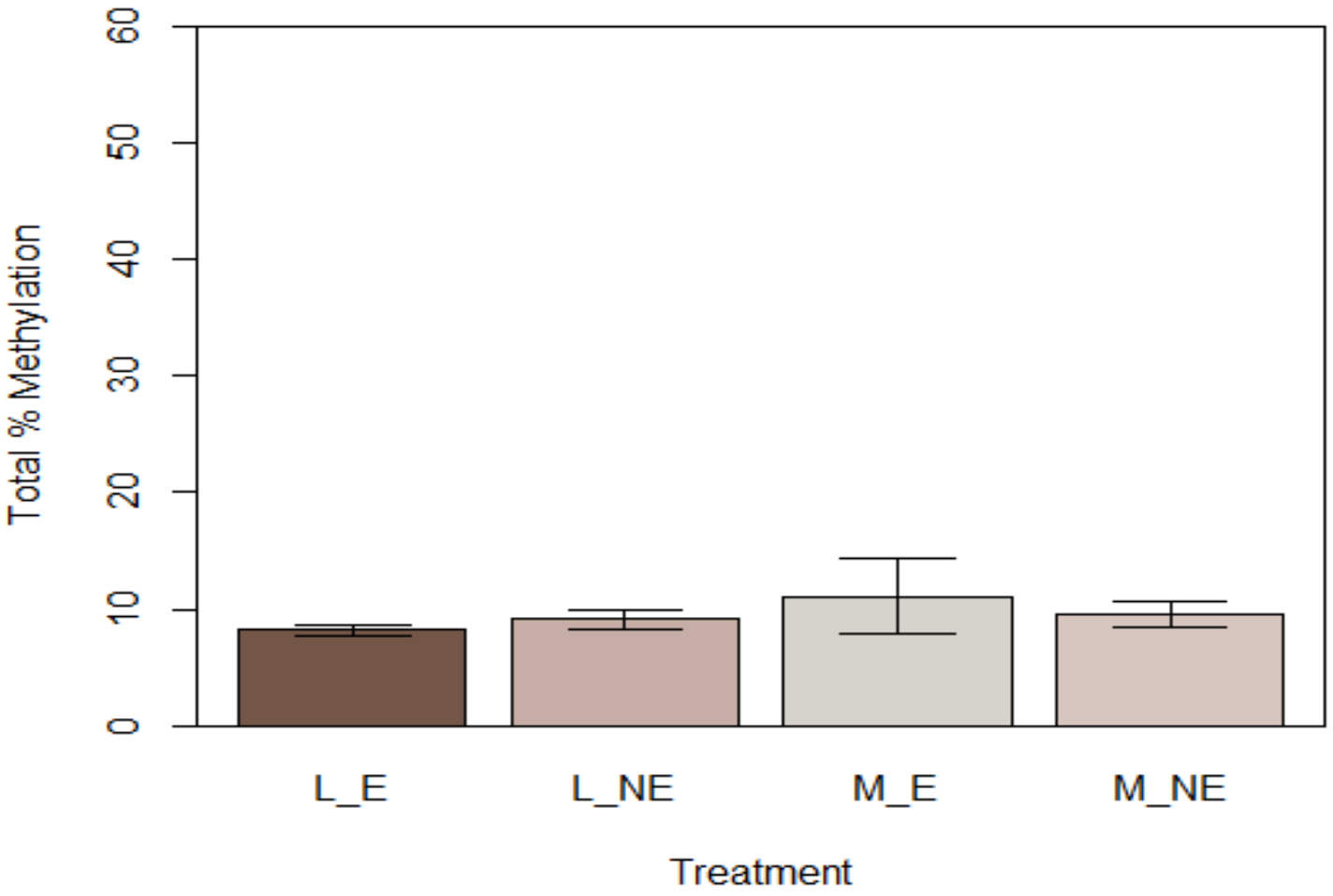

B)

REFERENCES

Akalin, A., Franke, V., Vlahoviček, K., Mason, C. E., & Schübeler, D. (2015). genomation: A toolkit to summarize, annotate and visualize genomic intervals. *Bioinformatics*, *31*(7), 1127–1129. https://doi.org/10.1093/bioinformatics/btu775

Akalin, A., Kormaksson, M., Li, S., Garrett-Bakelman, F. E., Figueroa, M. E., Melnick, A., & Mason, C. E. (2012). methylKit: A comprehensive R package for the analysis of genome-wide DNA methylation profiles. *Genome Biology*, *13*(10), R87. https://doi.org/10.1186/gb-2012-13-10-r87

Ashburner, M., Ball, C. A., Blake, J. A., Botstein, D., Butler, H., Cherry, J. M., Davis, A. P., Dolinski, K., Dwight, S. S., Eppig, J. T., Harris, M. A., Hill, D. P., Issel-Tarver, L., Kasarskis, A., Lewis, S., Matese, J. C., Richardson, J. E., Ringwald, M., Rubin, G. M., & Sherlock, G. (2000). Gene Ontology: Tool for the unification of biology. *Nature Genetics*, *25*(1), 25–29. https://doi.org/10.1038/75556

Babraham Bioinformatics—Bismark Bisulfite Read Mapper and Methylation Caller. (n.d.). Retrieved August 22, 2023, from https://www.bioinformatics.babraham.ac.uk/projects/bismark/

Beocat. (2021, October 22). [Educational institution]. Kansas State University. https://support.beocat.ksu.edu/BeocatDocs/index.php?title=Main_Page

Blackledge, N. P., & Klose, R. J. (2011). CpG island chromatin. *Epigenetics*, *6*(2), 147–152. https://doi.org/10.4161/epi.6.2.13640

Blake, L., Roux, J., Hernando-Herraez, I., Banovich, N., Perez, R., Hsiao, C., Eres, I., Cuevas, C., Marques-Bonet, T., & Gilad, Y. (2020). A comparison of gene expression and DNA

methylation patterns across tissues and species. *Cold Spring Harbor Laboratory Press*. www.genome.org/cgi/doi/10.1101/gr.254904.119

Bolger, A. M., Lohse, M., & Usadel, B. (2014). Trimmomatic: A flexible trimmer for Illumina sequence data. *Bioinformatics*, *30*(15), 2114–2120. https://doi.org/10.1093/bioinformatics/btu170

Burrell, A. S., Disotell, T. R., & Bergey, C. M. (2015). The use of museum specimens with high-throughput DNA sequencers. *Journal of Human Evolution*, *79*, 35–44. https://doi.org/10.1016/j.jhevol.2014.10.015

Cain, J. A., Montibus, B., & Oakey, R. J. (2022). Intragenic CpG Islands and Their Impact on Gene Regulation. *Frontiers in Cell and Developmental Biology*, *10*. https://www.frontiersin.org/articles/10.3389/fcell.2022.832348

Cook, J. A., & Light, J. E. (2019). The emerging role of mammal collections in 21st century mammalogy. *Journal of Mammalogy*, *100*(3), 733–750. https://doi.org/10.1093/jmammal/gyy148

Crossman, C. A., Barrett-Lennard, L. G., & Frasier, T. R. (2021). An example of DNA methylation as a means to quantify stress in wildlife using killer whales. *Scientific Reports*, *11*(1), Article 1. https://doi.org/10.1038/s41598-021-96255-1

De Paoli-Iseppi, R., Deagle, B. E., McMahon, C. R., Hindell, M. A., Dickinson, J. L., & Jarman, S. N. (2017). Measuring Animal Age with DNA Methylation: From Humans to Wild Animals. *Frontiers in Genetics*, *8*. https://www.frontiersin.org/articles/10.3389/fgene.2017.00106

Fan, S., & Zhang, X. (2009). CpG island methylation pattern in different human tissues and its correlation with gene expression. *Biochemical and Biophysical Research Communications*, *383*(4), 421–425. https://doi.org/10.1016/j.bbrc.2009.04.023

FastQC. (n.d.). Retrieved September 28, 2023, from https://www.illumina.com/products/by-type/informatics-products/basespace-sequence-hub/apps/fastqc.html

Francis, D. D., & Meaney, M. J. (1999). Maternal care and the development of stress responses. *Current Opinion in Neurobiology*, *9*(1), 128–134. https://doi.org/10.1016/S0959-4388(99)80016-6

Gu, H., Smith, Z. D., Bock, C., Boyle, P., Gnirke, A., & Meissner, A. (2011). Preparation of reduced representation bisulfite sequencing libraries for genome-scale DNA methylation profiling. *Nature Publishing Group*, *6*(4), 468–482. https://doi.org/10.1038/nprot.2010.190

Hahn, E. E., Grealy, A., Alexander, M., & Holleley, C. E. (2020). Museum Epigenomics: Charting the Future by Unlocking the Past. *Trends in Ecology & Evolution*, *35*(4), 295–300. https://doi.org/10.1016/j.tree.2019.12.005

Horvath, S., Haghani, A., Zoller, J. A., Naderi, A., Soltanmohammadi, E., Farmaki, E., Kaza, V., Chatzistamou, I., & Kiaris, H. (2021). Methylation studies in Peromyscus: Aging, altitude adaptation, and monogamy. *GeroScience*. https://doi.org/10.1007/s11357-021-00472-5

Hughes, A. L., Kelley, J. R., & Klose, R. J. (2020). Understanding the interplay between CpG island-associated gene promoters and H3K4 methylation. *Biochimica et Biophysica Acta. Gene Regulatory Mechanisms*, *1863*(8), 194567. https://doi.org/10.1016/j.bbagrm.2020.194567

Husby, A. (2022). Wild epigenetics: Insights from epigenetic studies on natural populations. *Proceedings of the Royal Society B: Biological Sciences*, *289*(1968), 20211633. https://doi.org/10.1098/rspb.2021.1633

Jin, B., Li, Y., & Robertson, K. D. (2011). DNA Methylation. *Genes & Cancer*, *2*(6), 607–617. https://doi.org/10.1177/1947601910393957

Kandi, V., & Vadakedath, S. (2015). Effect of DNA Methylation in Various Diseases and the Probable Protective Role of Nutrition: A Mini-Review. *Cureus*, *7*(8), e309. https://doi.org/10.7759/cureus.309

Kansas Mammal Atlas: White-footed Mouse. (2017, July 13). [Educational institution]. Fort Hays State Unviersity. https://webapps.fhsu.edu/ksfauna

Kolberg, L., Raudvere, U., Kuzmin, I., Adler, P., Vilo, J., & Peterson, H. (2023). g:Profiler—Interoperable web service for functional enrichment analysis and gene identifier mapping (2023 update). *Nucleic Acids Research*, *51*(W1), W207–W212. https://doi.org/10.1093/nar/gkad347

Konietschke, F., Noguchi, K., & Rubarth, K. (2019). *nparcomp: Multiple Comparisons and Simultaneous Confidence Intervals* (3.0) [Computer software]. https://cran.r-project.org/web/packages/nparcomp/index.html

Krueger, F., & Andrews, S. R. (2011). Bismark: A flexible aligner and methylation caller for Bisulfite-Seq applications. *Bioinformatics*, *27*(11), 1571–1572. https://doi.org/10.1093/bioinformatics/btr167

Lackey, J. A., Huckaby, D. G., & Ormiston, B. G. (1985). Peromyscus leucopus. *Mammalian Species*, *247*, 1–10. https://doi.org/10.2307/3503904

Lakshminarasimhan, R., & Liang, G. (2016). The Role of DNA Methylation in Cancer. *Advances in Experimental Medicine and Biology, 945*, 151–172. https://doi.org/10.1007/978-3-319-43624-1_7

Langmead, B., & Salzberg, S. L. (2012). Fast gapped-read alignment with Bowtie 2. *Nature Methods*, *9*(4), Article 4. https://doi.org/10.1038/nmeth.1923

Laubach, Z. M., Faulk, C. D., Dolinoy, D. C., Montrose, L., Jones, T. R., Ray, D., Pioon, M. O., & Holekamp, K. E. (2019). Early life social and ecological determinants of global DNA methylation in wild spotted hyenas. *Molecular Ecology*, *28*(16), 3799–3812. https://doi.org/10.1111/mec.15174

Lennard, L. (2010). *Methyltransferase—An overview | ScienceDirect Topics*. Science Direct. https://www.sciencedirect.com/topics/neuroscience/methyltransferase

Lim, W.-J., Kim, K. H., Kim, J.-Y., Jeong, S., & Kim, N. (2019). Identification of DNA-Methylated CpG Islands Associated With Gene Silencing in the Adult Body Tissues of the Ogye Chicken Using RNA-Seq and Reduced Representation Bisulfite Sequencing. *Frontiers in Genetics*, *10*. https://www.frontiersin.org/articles/10.3389/fgene.2019.00346

Lindblad-Toh, K. (2020). What animals can teach us about evolution, the human genome, and human disease. *Upsala Journal of Medical Sciences, 125*(1), 1–9. https://doi.org/10.1080/03009734.2020.1722298

Lokk, K., Modhukur, V., Rajashekar, B., Märtens, K., Mägi, R., Kolde, R., Koltšina, M., Nilsson, T. K., Vilo, J., Salumets, A., & Tõnisson, N. (2014). DNA methylome profiling of human tissues identifies global and tissue-specific methylation patterns. *Genome Biology*, *15*(4), 3248. https://doi.org/10.1186/gb-2014-15-4-r54

Lutgen, D., & Burri, R. (2022, June 19). *DNA extraction protocol for historical toe pad samples from birds*. Protocols.Io. https://www.protocols.io/view/dna-extraction-protocol-for-historical-toe-pad-sam-bm4mk8u6

Macartney-Coxson, D., Cameron, A. M., Clapham, J., & Benton, M. C. (2020). DNA methylation in blood—Potential to provide new insights into cell biology. *PLoS ONE*, *15*(11), e0241367. https://doi.org/10.1371/journal.pone.0241367

Maksimovic, J., Oshlack, A., & Phipson, B. (2021). Gene set enrichment analysis for genome-wide DNA methylation data. *Genome Biology*, *22*(1), 173. https://doi.org/10.1186/s13059-021-02388-x

Martin, C., & Zhang, Y. (2007). Mechanisms of epigenetic inheritance. *Current Opinion in Cell Biology*, *19*(3), 266–272. https://doi.org/10.1016/j.ceb.2007.04.002

Model Organisms | NIH Center for Scientific Review. (n.d.). Retrieved September 29, 2023, from https://public.csr.nih.gov/FAQs/ReviewersFAQs/ModelOrganisms

Moore, L. D., Le, T., & Fan, G. (2013). DNA Methylation and Its Basic Function. *Neuropsychopharmacology*, *38*(1), Article 1. https://doi.org/10.1038/npp.2012.112

Murgatroyd, C., Patchev, A., Wu, Y., Micale, V., Bockmühl, Y., Fischer, D., Holsboer, F., Wotjak, C., Almeida, O., & Spengler, D. (2009). Dynamic DNA methylation programs persistent adverse effects of early-life stress. *Nature Neuroscience*, *12*, 1559–1566. https://doi.org/10.1038/nn.2436

Nachtomy, O., Shavit, A., & Yakhini, Z. (2007). Gene expression and the concept of the phenotype. *Studies in History and Philosophy of Science Part C: Studies in History and Philosophy of Biological and Biomedical Sciences*, *38*(1), 238–254. https://doi.org/10.1016/j.shpsc.2006.12.014

Peromyscus leucopus Genome Assembly. (2020, October 2). NCBI. https://www.ncbi.nlm.nih.gov/assembly/GCF_004664715.2

Primer3. (n.d.). Retrieved October 12, 2023, from https://primer3.org/

R Core Team. (2023). *R: A Language and Environment for Statistical Computing* [Computer software]. R Foundation for Statistical Computing. https://www.R-project.org/

Robeck, T. R., Haghani, A., Fei, Z., Lindemann, D. M., Russell, J., Herrick, K. E. S., Montano, G., Steinman, K. J., Katsumata, E., Zoller, J. A., & Horvath, S. (2023). Multi-tissue DNA methylation aging clocks for sea lions, walruses and seals. *Communications Biology*, *6*(1), Article 1. https://doi.org/10.1038/s42003-023-04734-0

Rubi, T., Knowles, L., & Dantzer, B. (2020). Museum epigenomics: Characterizing cytosine methylation in historic museum specimens. *Molecular Ecology Resources*, *20*(5), 1161–1170. https://doi.org/10.1101/1755-0998.13115

Shi, Y. (2021). *Sex and tissue specific DNA methylation patterns in the house sparrow (Passer domesticus)* [Uppsala University]. http://www.diva-portal.org/smash/get/diva2:1563799/FULLTEXT01.pdf

Tamaru, H. (2010). Confining euchromatin/heterochromatin territory: Jumonji crosses the line. *Genes & Development*, *24*(14), 1465–1478. https://doi.org/10.1101/gad.1941010

UCSC Genome Browser. (n.d.). Retrieved September 3, 2023, from http://genome.ucsc.edu/cgi-bin/hgGateway?hgsid=1698780776_O961YFcFyWMMuIYzyZ8eVybWbLt8

Warnes, G. R., Bolker, B., Bonebakker, L., Gentleman, R., Huber, W., Liaw, A., Lumley, T., Maechler, M., Magnusson, A., Moeller, S., Schwartz, M., Venables, B., & Galili, T. (2022). *gplots: Various R Programming Tools for Plotting Data* (3.1.3) [Computer software]. https://cran.r-project.org/web/packages/gplots/index.html

Weyrich, A., Benz, S., Karl, S., Jeschek, M., Jewgenow, K., & Fickel, J. (2016). Paternal heat exposure causes DNA methylation and gene expression changes of Stat3 in Wild guinea pig sons. *Ecology and Evolution*, *6*(9), 2657–2666. https://doi.org/10.1002/ece3.1993

Wickham, H., Chang, W., Henry, L., Pedersen, T. L., Takahashi, K., Wilke, C., Woo, K., Yutani, H., Dunnington, D., Posit, & PBC. (2023). *ggplot2: Create Elegant Data Visualisations Using the Grammar of Graphics* (3.4.4) [Computer software]. https://cran.r-project.org/web/packages/ggplot2/index.html

Wright, P. G. R., Mathews, F., Schofield, H., Morris, C., Burrage, J., Smith, A., Dempster, E. L., & Hamilton, P. B. (2018). Application of a novel molecular method to age free-living wild Bechstein's bats. *Molecular Ecology Resources*, *18*(6), 1374–1380. https://doi.org/10.1111/1755-0998.12925

Zhang, B., Zhou, Y., Lin, N., Lowdon, R. F., Hong, C., Nagarajan, R. P., Cheng, J. B., Li, D., Stevens, M., Lee, H. J., Xing, X., Zhou, J., Sundaram, V., Elliott, G., Gu, J., Shi, T., Gascard, P., Sigaroudinia, M., Tlsty, T. D., … Wang, T. (2013). Functional DNA methylation differences between tissues, cell types, and across individuals discovered using the M&M algorithm. *Genome Research*, *23*(9), 1522–1540. https://doi.org/10.1101/gr.156539.113

Zhang, J., Fu, H., & Xu, Y. (2021). Age Prediction of Human Based on DNA Methylation by Blood Tissues. *Genes*, *12*(6), Article 6. https://doi.org/10.3390/genes12060870

Fort Hays State University
FHSU Scholars Repository
Non-Exclusive License Author Agreement

I hereby grant Fort Hays State University an irrevocable, non-exclusive, perpetual license to include my thesis ("the Thesis") in *FHSU Scholars Repository*, FHSU's institutional repository ("the Repository").

I hold the copyright to this document and agree to permit this document to be posted in the Repository, and made available to the public in any format in perpetuity.

I warrant that the posting of the Thesis does not infringe any copyright, nor violate any proprietary rights, nor contains any libelous matter, nor invade the privacy of any person or third party, nor otherwise violate FHSU Scholars Repository policies.

I agree that Fort Hays State University may translate the Thesis to any medium or format for the purpose of preservation and access. In addition, I agree that Fort Hays State University may keep more than one copy of the Thesis for purposes of security, back-up, and preservation.

I agree that authorized readers of the Thesis have the right to use the Thesis for non-commercial, academic purposes, as defined by the "fair use" doctrine of U.S. copyright law, so long as all attributions and copyright statements are retained.

To the fullest extent permitted by law, both during and after the term of this Agreement, I agree to indemnify, defend, and hold harmless Fort Hays State University and its directors, officers, faculty, employees, affiliates, and agents, past or present, against all losses, claims, demands, actions, causes of action, suits, liabilities, damages, expenses, fees and costs (including but not limited to reasonable attorney's fees) arising out of or relating to any actual or alleged misrepresentation or breach of any warranty contained in this Agreement, or any infringement of the Thesis on any third party's patent, trademark, copyright or trade secret.

I understand that once deposited in the Repository, the Thesis may not be removed.

Thesis: METHYLATION PATTERNS ACROSS TISSUE TYPE AND TIME IN PEROMYSCUS LEUCOUPUS: A TARGETED MUSEUM STUDY

Author: Loryn Smith

Signature: Loryn Smith

Date: 11/17/2023